Evaluation of CH4MOD$_{wetland}$ and TEM models used to estimate global CH_4 emissions from natural wetlands

Tingting Li[1,2], Yanyu Lu[3], Lingfei Yu[4], Wenjuan Sun[4], Qing Zhang[1], Wen Zhang[1], Guocheng Wang[1], Zhangcai Qin[2,5], Lijun Yu[1], Hailing Li[1], Ran Zhang[6]

[1]LAPC, Institute of Atmospheric Physics, Chinese Academy of Sciences, Beijing 100029, China
[2]Southern Marine Science and Engineering Guangdong Laboratory (Zhuhai), Zhuhai 519000, China
[3]Anhui Climate Center, Hefei 230031, China
[4]Institute of Botany, Chinese Academy of Sciences, Beijing 100049, China
[5]School of Atmospheric Sciences, Sun Yat-sen University, Guangzhou 510245, China
[6] CCRC, Institute of Atmospheric Physics, Chinese Academy of Sciences, Beijing 100029, China

Correspondence to: Yanyu Lu (ahqxlyy@163.com), Lingfei Yu(yulf@ibcas.ac.cn)

Abstract

Wetlands are the largest and most uncertain natural sources of atmospheric methane (CH_4). Several process-based models have been developed to quantify the magnitude and estimate spatial and temporal variations in CH_4 emissions from global wetlands. Reliable models are required to estimate global wetland CH_4 emissions. This study aimed to test two process-based models, $CH4MOD_{wetland}$ and TEM, against the CH_4 flux measurements of marsh, swamp, peatland and coastal wetland sites across the world; specifically, model accuracy and generality were evaluated for different wetland types and in different continents, and then the global CH_4 emissions from 2000 to 2010 were estimated. Both models showed similar high correlations with the observed seasonal/annual total CH_4 emissions, and the regression of the observed versus computed total seasonal/annual CH_4 emissions resulted in R^2 values of 0.81 and 0.68 for $CH4MOD_{wetland}$ and the TEM, respectively. The $CH4MOD_{wetland}$ produced accurate predictions for marshes, peatlands, swamps and coastal wetlands, with model efficiency (EF) values of 0.22, 0.52, 0.13 and 0.72, respectively. The TEM produced good predictions for peatlands and swamps, with EF values of 0.69 and 0.74, respectively, but it could not accurately simulate marshes and coastal wetlands ($EF<0$). There was a good correlation between the simulated CH_4 fluxes and the observed values on most continents. However, $CH4MOD_{wetland}$ showed no correlation with the observed values in South America and Africa. The TEM showed no correlation with the observations in Europe. The global CH_4 emissions for the period 2000–2010 were estimated to be 105.31±2.72 Tg yr^{-1} by $CH4MOD_{wetland}$ and 134.31±0.84 Tg yr^{-1} by the TEM. Both models simulated a similar spatial distribution of CH_4 emissions globally and on different continents. Marshes contribute 36–39% of global CH_4 emissions. Lakes/rivers and swamps are the second and third greatest contributors, respectively. Other wetland types account for only approximately 20% of global emissions. Based on the model applicability, if we use the more accurate model, i.e., the one that performs best as evidenced by a higher model efficiency and a lower model bias, to estimate each continent/wetland type, we obtain a new assessment of 116.99–124.74 Tg yr^{-1} for the global CH_4 emissions for the period 2000–2010. Our results imply that performance at a global scale may conceal model uncertainty. Efforts should be made to improve model accuracy for different wetland types and regions, particularly hotspot regions, to reduce the uncertainty in global assessments.

1 Introduction

Atmospheric methane (CH_4) is the second most prevalent human-induced greenhouse gas (GHG) after carbon dioxide (CO_2). Its radiative forcing effect is 28 times greater than that of CO_2 on a 100-year horizon (Myhre et al., 2013). The radiative forcing attributed to CH_4 has been re-evaluated by the Intergovernmental Panel on Climate Change (IPCC)'s 5th Assessment Report (AR5) and was reported to be almost twice as high as the value reported in the 4th Assessment Report (AR4), with values of 0.97 W m^{-2} versus 0.48 W m^{-2}, respectively (Myhre et al., 2013). This estimate considers that the emission of CH_4 leads to an increase in ozone production, stratospheric water vapor and CO_2, which can affect its own lifetime (Boucher et al., 2009; Myhre et al., 2013; Shindell et al., 2012).

The growth rate of the atmospheric CH_4 concentration has varied in different historical periods. There was an exponential increase from preindustrial times to the 1980s. The growth rate decreased after the 1980s and was close to zero from 1999 to 2006; then, the growth rate resumed strong growth in the period of 2007-2017 (Dlugokencky et al., 2009, 2016; Nisbet et al., 2019). However, the causes that drive the variations in growth rate remain unclear due to the uncertainties in estimating CH_4 emissions and sinks (Ghosh et al., 2015; Saunois et al., 2016; Nisbet et al., 2019; Dalsøren et al., 2016).

Integrated at the global scale, wetlands are the largest and most uncertain source of CH_4 emitted to the atmosphere (Kirschke et al., 2013; Saunois et al., 2016). These emissions represent approximately 30% of the total CH_4 input (Saunois et al., 2016). Bottom-up and top-down approaches are popular methods for estimating global CH_4 emissions from natural wetlands. Top-down approaches are based on inverse models (e.g., Bousquet et al., 2006; Fraser et al., 2013; Meirink et al., 2008; Tsuruta et al., 2017; Bruhwiler et al., 2014), which determine 'optimal' surface fluxes that best fit atmospheric CH_4 observations given an atmospheric transport model including chemistry, prior estimates of fluxes, and their uncertainties (Kirschke et al., 2013). Bottom-up approaches use process-based models that describe the relationship between the environmental factors and the processes of CH_4 production, oxidation and emission using mathematical equations (e.g., Li et al., 2010; Zhu et al., 2013; Zhang et al., 2002; Zhu et al., 2014; Walter and Heimann, 2000; Tian et al., 2015; Riley et al., 2011; Meng et al., 2012; Zhuang et al., 2006).

Recent studies related to the bottom-up approach have used an ensemble of process-based models driven by the same climate forcing to estimate the global CH_4 emissions from natural wetlands. For example, the Wetland and Wetland CH_4 Intercomparison of Models Project (WETCHIMP) used ten land surface models and estimated global CH_4 emissions of 190 ± 76 Tg CH_4 yr^{-1} for the 1993–2004 period (Melton et al., 2013). In the following year, Kirschke et al. (2013) assessed a large emission range of 142–287 Tg CH_4 yr^{-1} from 1980 to 2010. Saunois et al. (2016) and Poulter et al. (2017) estimated global emissions of 153–227 Tg CH_4 yr^{-1} for the decade 2003–2012 and 184 ± 22 Tg CH_4 yr^{-1} for the decade 2000–2012 using ensemble process-based models (Poulter et al., 2017). Saunois et al. (2016) suggested that approximately 70% of the uncertainty was due to model structures and parameters.

Natural wetland ecosystems are greatly heterogeneous on a global scale. Wetlands vary widely by continent with respect to area and type (Kingsford et al., 2016; Keddy, 2010). Some wetland types have higher emissions, while some emit less CH_4; this difference is because the processes of controls on CH_4 cycling differ among wetland types (Bridgham et al., 2013). For example, sedge-dominated marsh or fen often emit higher CH_4 fluxes because sedges can increase methanogenic substrates as part of their plant productivity and promote CH_4 transportation through their soft aerenchyma and lacunae tissues (McEwing et al., 2015; Jitka et al., 2017; Bhullar et al., 2013; Joabsson and Christensen, 2001; Kwon et al., 2017; King et al., 2002; Chanton, 2005). Bog soils with anaerobic incubations emit little CH_4 due to the particularly high CO_2:CH_4 ratios of the end products of anaerobic carbon (Bridgham et al., 1998; Galand et al., 2010; Keller and Bridgham, 2007). Coastal wetlands with high salinity usually emit less CH_4 than other wetlands because the sulfate in seawater inhibits CH_4 production (Bartlett et al., 1985; Delaune et al., 1983; Li et al., 2016; Poffenbarger et al., 2011).

Model evaluation is a core part of model development and testing (Bennett et al., 2013). Based on the model evaluation, the modeler must be confident that the model will fulfill its purpose (Bennett et al., 2013; Rykiel, 1996). If applying process-based models for global-scale CH_4 estimations, it is necessary to evaluate its performance in different wetland types and regions. This process is also helpful for confirming the source of uncertainties and improving the model. However, previous studies have always focused on global assessments and have overlooked model performance in different wetland types or regions, which may have induced high uncertainties (Poulter et al., 2017; Saunois et al., 2016; Kirschke et al., 2013; Melton et al., 2013). $CH4MOD_{wetland}$ (Li et al., 2010) and the Terrestrial Ecosystem Model (TEM) (Zhuang et al., 2004; Melillo et al., 1993; Zhuang et al., 2007; Zhuang et al., 2013) are two established process-based models that can be used to simulate regional and global wetland CH_4 emissions.

Both models have been validated at specific sites (Zhu et al., 2013; Li et al., 2010; Li et al., 2017). However, we do not have information on the accuracy and applicability of the models for different wetland types and on different continents. The objectives of this study were to comprehensively evaluate the model performances of $CH4MOD_{wetland}$ and the TEM for different wetland types and on different continents and then to use the models to estimate global CH_4 emissions from natural wetlands.

2 Methods and Materials

The performance evaluation should clearly depend on the model objectives (Bennett et al., 2013). The models considered in this study aim to estimate the annual emissions from global wetlands. Therefore, the accuracy and applicability of the model in simulating annual CH_4 emissions for different wetland types and continents are very important in a performance evaluation. Several process-based models have been developed in recent decades (Xu et al., 2016). Some models are simple semiempirical models that focus on the biochemical processes of CH_4 production, oxidation and emission, e.g., Walter's model (Walter et al., 1996; Walter and Heimann, 2000), CASA (Potter, 1997) and $CH4MOD_{wetland}$ (Li et al., 2010). This kind of model requires simple inputs and parameters and is easily extrapolated to a regional scale. Other models are based on more complex land ecosystem models coupled to the CH_4 processes module, such as CLM4Me, ORCHIDEE, SDGVM and TEM. These models describe complex ecosystem processes require more inputs and parameters. In this study, we chose $CH4MOD_{wetland}$ and the TEM to compare the model performance of a simple easy-to-run model and a sophisticated land ecosystem model. Moreover, both models have been validated at the site scale, but no comprehensive accuracy analysis in different continents or for various wetland types has been done before. We collected CH_4 flux measurements from 43 wetlands spanning the main wetland types in the world from peer-reviewed literature (Table 1). A set of statistical methods was used to comprehensively evaluate the performance of $CH4MOD_{wetland}$ and the TEM in different wetland types and on different continents. Finally, we extrapolated both models to estimate the global CH_4 emissions from 2000 to 2010.

2.1 Model overview

2.1.1 CH4MOD$_{wetland}$

The CH4MOD$_{wetland}$ model is a process-based biogeophysical model used to simulate the processes of CH_4 production, oxidation and emission from natural wetlands (Li et al., 2010). The model was established based on CH4MOD, which is used to predict CH_4 emissions from rice paddies (Huang et al., 1998; Huang et al., 1997). In CH4MOD$_{wetland}$, we focused on the differences in the supply of methanogenic substrates between natural wetlands and rice paddies. Methanogenic substrates are derived from root exudates, the decomposition of plant litter and soil organic matter. The methane production rates were determined based on the methanogenic substrates and the influence of environmental factors, including soil temperature, soil texture and soil redox potential. Additionally, we incorporated the influence of salinity on CH_4 production to improve the model performance for coastal wetlands (Li et al., 2016). Inputs to the CH4MOD$_{wetland}$ model include the daily air/soil temperature, water table depth, annual aboveground net primary productivity (ANPP), soil sand fraction, soil organic matter, bulk density and soil salinity. The outputs are the daily and annual CH_4 production and emissions. We used the TOPMODEL hydrological model to simulate the water table depth as the inputs of CH4MOD$_{wetland}$ (Bohn et al., 2007; Li et al., 2015; Li et al., 2019; Zhu et al., 2013; Beven and Kirkby, 1979).

The main parameters that must be calibrated in CH4MOD$_{wetland}$ include the vegetation index (*VI*), which was used to quantify the different capacities for producing root exudates of the various plant species, the fraction of plant-mediated transport available (T_{veg}), the fraction of CH_4 oxidized during plant-mediated transport (P_{ox}), the proportion of belowground net primary productivity (*BNPP*) to the total net primary productivity (*NPP*) (f_r), the fraction of nonstructural component in plant litter (F_N) (Table S1) and the empirical constant of the influence of salinity. The model parametrization and main parameters are described in Supplementary Material S1.

2.1.2 TEM

The TEM is another process-based biogeochemical model that couples carbon, nitrogen, water, and heat processes in terrestrial ecosystems to simulate ecosystem carbon and nitrogen dynamics (Melillo et al., 1993; Zhuang et al., 2007; Zhuang et al., 2013). The methane dynamics module was first coupled within the TEM by Zhuang et al. (2004) to explicitly simulate the process of methane production (methanogenesis), oxidation (methanotrophy) and transport between the soil and the atmosphere. Methane production is assumed to occur only in saturated zones and is regulated by organic substrate, soil thermal conditions, soil pH, and soil redox potentials; methane oxidation, which occurs in the unsaturated zone, depends on the soil methane and oxygen concentrations, temperature, moisture and redox potential. Methane transport is described by three pathways in the TEM: (1) diffusion through the soil profile, (2) plant-aided transport, and (3) ebullition. The TEM has also been coupled with TOPMODEL (Zhu et al., 2013). The model calibration of the TEM is well documented in Supplementary Material S2 and Table S2.

2.2 Site information and data sources

2.2.1 Site information

We collected 43 wetland sites across the world (Table 1). The wetland sites included 6 marsh sites, 25 peatland sites, 8 swamp sites and 4 coastal wetland sites. Among the wetland sites, 7 sites are distributed in Europe (EU), 11 sites are distributed in Asia (AS), 2 sites are distributed in Africa (AF), 4 sites are distributed in South America (SA) and 19 sites are distributed in North America (NA). The observations were from the late 1980s to the 2010s. The observation periods covered either a growing season or a whole year (Table 1). We calculated the total amount of CH_4 emissions during the growing season or the whole year as the observed seasonal/annual CH_4 emissions. For most of the wetland sites, the total amount of seasonal/annual CH_4 emissions during the observation period was calculated by summing the daily observations. Gaps in the CH_4 emission measurements were filled by linear interpolation between two adjacent days of observations. For a few wetland sites, the observed seasonal/annual CH_4 emissions were directly obtained from the literature. More details about the location, vegetation and observation periods are described in Table 1.

2.2.2 Wetland map

The global wetland distributions of different wetland types were based on the Global Lakes and Wetlands Database (GLWD-3) (http://www.wwfus.org/science/data.cfm) (Lehner and Döll, 2004) (Fig.

1). According to GLWD-3, the wetland types include 1. lakes, 2. reservoirs, 3. rivers (we combined lakes, reservoirs and rivers as a single wetland type, hereafter referred to as lakes/rivers), 4. freshwater marsh and floodplain (hereafter referred to as marsh), 5. swamp forest and flooded forest (hereafter referred to as swamp), 6. coastal wetland, 7. saline wetland (we combined coastal wetland and saline wetland as a single wetland type, hereafter referred to as coastal wetland), 8. bog, fen and mire (hereafter referred to as peatland), 9. intermittent wetland and 10. no-specific wetland. All of the observed sites (Table 1) are distributed on the wetland map (Fig. 1).

The global wetland area (excluding rivers) was estimated by the "Global Review of Wetland Resources and Priorities for Wetland Inventory (GRoWI)" as 530-570 M ha (Spiers, 1999). We used an average value, as the wetland area excluded rivers in this study. The global wetland area of rivers was based on GLWD-3. Therefore, we assumed that the global wetland area was 584 M ha, which represented the wetland area for the period from 2000 to 2010. The cartography-based GLWD-3 data provide a global distribution of natural wetlands at a 30-second resolution. Then, we aggregated the merged map up to $0.5° \times 0.5°$ (latitude × longitude) grids. The wetland area (excluding rivers) in each pixel was adjusted by the ratio of the global wetland area estimated by GRoWI and by GLWD-3.

2.2.3 Driver data

The input climate data for the models include the daily air temperature, precipitation, cloudiness and vapor pressure. The historical daily climate data were developed from the latest monthly data sets of the Climatic Research Unit (CRU TS 3.10) of the University of East Anglia in the United Kingdom (Harris et al., 2014).

The soil properties needed by the $CH4MOD_{wetland}$ model include soil texture (percentage of sand in the soil), bulk density, soil organic carbon content, soil temperature and soil moisture. The additional information needed by the TEM includes the percentage of silt and clay in the soil, soil pH and site elevation. The soil texture data were derived from the soil map of the Food and Agriculture Organization (FAO) (FAO, 2012). The soil organic carbon content and the reference bulk density of wetland soils were retrieved from the Harmonized World Soil Database (HWSD) (FAO, 2008) by masking the HWSD with the Global Lakes and Wetlands Database (GLWD) (Lehner and Döll, 2004). The daily soil temperature data were estimated by the TEM from spatially interpolated climate data. The daily soil moisture driving

$CH4MOD_{wetland}$ coupled with TOPMODEL was developed from the monthly dataset (http://www.cpc.ncep.noaa.gov/soilmst/leaky_glb.htm) by temporal linear interpolation (Fan and van den Dool, 2004). The soil pH was also derived from the global soil property dataset of the International Geosphere-Biosphere Programme (IGBP) (Carter and Scholes, 2000).

The vegetation map of the IGBP was referenced to specify the vegetation parameters for $CH4MOD_{wetland}$ (Table S1) and the TEM. The map was derived from the IGBP Data and Information System (DIS) DISCover Database (Belward et al., 1999; Loveland et al., 2000). The 1 km × 1 km DISCover dataset was reclassified into the TEM vegetation classification scheme and then aggregated into 0.5° × 0.5° grids. The annual ANPP used to drive $CH4MOD_{wetland}$ was from the output of the TEM.

For $CH4MOD_{wetland}$, a high-resolution topographic wetness index dataset (Marthews et al., 2015) was used to calculate the changes in the water table. Global salinity data were obtained from the World Ocean Atlas 2009 (Antonov et al., 2010). We also used 1 km × 1 km global elevation data derived from the Shuttle Radar Topography Mission (SRTM) (Farr et al., 2007). The above data were resampled to 0.5° × 0.5° grids to match the resolution of the other input data.

2.3 Model evaluation

We compared the observed seasonal/annual CH_4 emissions from the wetland sites (Table 1) and the simulated CH_4 emissions at the 0.5°×0.5° grid scale for the same period (described in Sect. 2.4). The statistics include the determination coefficient (R^2), the root mean square error (RMSE), the mean deviation (RMD), the model efficiency (EF) and the coefficient of determination (CD) were used to evaluate model performance on a global scale, a continental scale and for each wetland type. Because of the limited number of sites in Africa and South America, we combined the two continents together.

Two simulations with the same RMSE values may not be considered equivalent because the distribution of the error among the sources may not be the same (Allen and Raktoe, 1981). We further analyzed the source of the model errors by decomposing it into three components: the mean bias from the modeling procedure (U_M), the errors due to regression (U_R) and the errors due to random disturbances (U_E) (Allen and Raktoe, 1981). The detailed description and the equations used to calculate these statistics are described in Supplementary Material S3.

2.4 Model extrapolation

CH4MOD$_{wetland}$ and the TEM were used to simulate the CH_4 emissions from global wetlands at a spatial resolution of 0.5°×0.5°. We established spatially explicit data for climate, soils, vegetation, land use and other environmental inputs at a 0.5°×0.5° spatial resolution to facilitate the models at the global scale. Both process-based models were conducted for the period of 1980–2010 in each pixel to simulate the temporal spatial variations in CH_4 fluxes. In this study, we focused only on the total CH_4 emissions for the period 2000–2010 because we assumed that the wetland map represented the distribution of natural wetlands during this period. The total CH_4 emissions from the natural wetlands, excluding the lakes/rivers in each pixel, were calculated as the product of the CH_4 fluxes and the gridded wetland area. To make an overall global/continental CH_4 emissions assessment, we evaluated the CH_4 emissions from lakes/rivers using the IPCC Tier 1 method based on the CH_4 emissions factor (IPCC, 1996) and the area of lakes/rivers in each pixel.

We aggregated the gridded values and obtained the annual mean CH_4 emissions from each wetland type and each continent by CH4MOD$_{wetland}$ combined with the IPCC Tier1 method (hereafter referred to as Method A) and the TEM combined with the IPCC Tier1 method (hereafter referred to as Method B). In addition, the two global assessments Method A and Method B, we made two other assessments of global CH_4 emissions by choosing the more accurate model (Method C and Method D). Based on the model performance evaluation (Sect. 2.3), we found a more accurate model for each wetland type and each continent. In the Method C approach, we chose the CH_4 emissions from each continent simulated by the more accurate model. In Oceania, we used the average simulated result by CH4MOD$_{wetland}$ and the TEM because there was no wetland site on this continent (Table 1). We summed the CH_4 emissions from all continents and made an assessment of the global CH_4 emissions. In the Method D approach, we chose the CH_4 emissions from marsh, peatland, swamp and coastal wetlands simulated by the more accurate model. The CH_4 emissions from intermittent wetlands and nonspecific wetlands were used as the average result by CH4MOD$_{wetland}$ and the TEM. The CH_4 emissions from lakes/rivers were based on the IPCC Tier 1 method. We summed the CH_4 emissions from all wetland types and assessed the global CH_4 emissions.

3. Results

3.1 Model evaluation

3.1.1 Model evaluation for global wetland sites

Fig. 2 shows the correlation of the modeled versus observed total amount of seasonal/annual CH_4 emissions by $CH4MOD_{wetland}$ (Fig. 2a) and the TEM (Fig. 2b). The regression of the observed versus computed total seasonal/annual CH_4 emissions by $CH4MOD_{wetland}$ (Fig. 2a) resulted in an R^2 of 0.81, with a slope of 1.17 and an intercept of -1.93 g m^{-2} (n=58, p<0.001). The regression of the observed versus computed total seasonal/annual CH_4 emissions by the TEM (Fig. 2b) resulted in an R^2 of 0.68, with a slope of 0.74 and an intercept of 4.77 g m^{-2} (n=58, p<0.001). These results indicated that the variations in the CH_4 emissions between sites and in different years could be delineated by both process-based models.

The statistics of the model performance of seasonal/annual CH_4 emissions (Table 2) indicated that both process-based models had the capability to simulate seasonal/annual CH_4 emissions from natural wetlands on a global scale (EF=0.65 for $CH4MOD_{wetland}$ and EF=0.68 for the TEM). However, a discrepancy still existed between the simulated and observed seasonal/annual CH_4 emissions (RMSE=67.00% for $CH4MOD_{wetland}$ and RMSE=63.58% for the TEM). For $CH4MOD_{wetland}$, the source of the errors was mainly from the regression error and random error, while for the TEM, the errors were mainly due to random disturbances (Table 2). Both models slightly overestimated the seasonal/annual CH_4 emissions on a global scale, with RMD values of ~4% (Table 2).

3.1.2 Model evaluation for different continents

We further analyzed the model predictions by $CH4MOD_{wetland}$ and the TEM among different continents (Fig. 3, Table 2). There was a good correlation between the simulated seasonal/annual CH_4 emissions and the observed values on most of the continents by the two models. The R^2 varied between 0.35 (Fig. 3e) and 0.94 (Fig. 3c) for $CH4MOD_{wetland}$ and between 0.26 (Fig. 3d) and 0.80 (Fig. 3h) for the TEM. The $CH4MOD_{wetland}$ model yielded more accurate predictions in Asia and North America, with EFs of 0.93 and 0.57, respectively (Fig. 3b and 3a, Table 2), than in South America and Africa (EF <0 in Table 2) (Fig. 3g). The TEM yielded more accurate predictions in North America and South

America/Africa than $CH4MOD_{wetland}$, with EF values of 0.76 and 0.53, but performed poorly in Europe (EF <0 in Table 2). $CH4MOD_{wetland}$ underestimated the observed emissions (RMD = -12.64%) in Asia and Europe (RMD = -29.91%) (Table 2). The TEM overestimated the CH_4 emissions in South America/Africa (RMD=15.31%) and slightly underestimated the CH_4 emissions in North America (RMD=-2.86%) (Table 1). Random error was the main contributor to the model errors in Asia and Europe in $CH4MOD_{wetland}$ and in Asia, North America, and South America/Africa in the TEM (Table 2). However, the regression error contributed most to the model errors in North America in $CH4MOD_{wetland}$ (Table 2).

3.1.3 Model evaluation for different wetland types

Fig. 4 shows the regressions of the simulated values against the observed total amount of seasonal/annual CH_4 emissions from the different wetland types. Regression analysis indicated that both models showed good performance in modeling seasonal/annual CH_4 emissions from the peatland sites (Fig. 4c and d). The TEM showed a better model efficiency and a lower RMSE and RMD than the $CH4MOD_{wetland}$ (Table 2) for peatland. For the other wetland types, $CH4MOD_{wetland}$ showed good performance in simulating the seasonal/annual CH_4 emissions from coastal wetlands (EF = 0.72), followed by marshes (EF = 0.22) and swamps (EF = 0.13) (Table 2). The TEM showed poor performance for the marsh sites (EF = -0.42) and coastal wetlands (EF = -2.26) (Table 2); however, it showed good performance for the swamp sites (EF = 0.74). There was no significant correlation ($p>0.05$) between the modeled and observed seasonal/annual CH_4 emissions from the marsh sites (Fig. 4b) and coastal wetland sites (Fig. 4h).

The errors by $CH4MOD_{wetland}$ were mainly due to the regression error for marsh and peatland (Table 2). For coastal wetlands, the model bias contributed 24%, the regression error contributed 30%, and the random error contributed 47% to the model errors (Table 2). The errors by the TEM were mainly due to the random error in peatland and swamps (Table 2).

3.2 Global CH_4 emissions from natural wetlands

3.2.1 Spatial pattern of global CH_4 emissions

The distribution of the simulated annual mean CH_4 fluxes and total CH_4 emissions for the period 2000–2010 showed similar patterns in $CH4MOD_{wetland}$ and the TEM (Fig. 5). The simulated latitudinal contributions of CH_4 fluxes were consistent between the two models (Supplementary material S4, Fig. 5a and 5b). Large emissions were found in South America, southern Africa and the border of Canada and the United States (Fig. 5c and 5d). The latitudinal sums of CH_4 emissions indicated that the strongest contribution came from the tropical zone (Fig. 5c and 5d). The latitudinal band of 10°S-0° contributed 22.77 Tg yr^{-1} and 23.23 Tg yr^{-1} CH_4 in $CH4MOD_{wetland}$ and the TEM, which accounted for 22% and 18% of the global emissions, respectively. A secondary large peak was simulated in the 40-50°N latitudinal band, with a value of 14.64 Tg yr^{-1} and 16.66 Tg yr^{-1} CH_4 according to $CH4MOD_{wetland}$ and the TEM, respectively. Generally, both models simulated a common decline in CH_4 emissions from lower latitudes to higher latitudes (Fig. 5c and 5d). The largest peak in CH_4 emissions was modeled in the 60-50°W meridional band, with values of 11.63 Tg yr^{-1} in $CH4MOD_{wetland}$ (Fig. 5c) and 13.83 Tg yr^{-1} in the TEM (Fig. 5d). This peak corresponded to the longitudes of the Amazon in South America. Both models simulated secondary peaks in the 30-40°E meridional band (Fig. 5c and 5d), which corresponded to the longitudes of the Congo in Africa.

3.2.2 CH_4 emissions from different continents and wetland types

Table 3 provides an overview of the CH_4 emissions from different continents and wetland types simulated by $CH4MOD_{wetland}$ and the TEM. A comparison of simulated CH_4 fluxes from different continents by $CH4MOD_{wetland}$ and the TEM showed that the three highest fluxes were modeled in South America, Africa and Asia (Table 3). The TEM simulated higher CH_4 fluxes in Europe than in North America, but the $CH4MOD_{wetland}$ simulations showed the opposite. For Oceania, the two models simulated similar fluxes.

Both models simulated the same sequence of CH_4 fluxes: swamp, marsh, intermittent wetland, no-specific wetland, coastal wetland, and peatland (Table 3). The simulated annual mean CH_4 fluxes from intermittent wetlands were almost equivalent in both models. For other wetland types, the TEM simulated higher CH_4 fluxes than the $CH4MOD_{wetland}$ model (Table 3). Both models simulated peak emissions in summer and lower emissions in winter for all wetland types except swamps (Fig. S1). Since large area of swamps distributed in southern hemisphere (Fig. 1), higher and lower CH_4 emissions were simulated during March to May and June to August, respectively (Fig. S1).

The global CH_4 emissions simulated by the TEM were 29 Tg yr^{-1} higher than those simulated by $CH4MOD_{wetland}$ (Table 3). This difference depended on the differences in the CH_4 fluxes and on the wetland area. The simulated results showed that half of this difference was attributed to marshes. South America contributed 30% to this difference because the simulated CH_4 fluxes differed greatly between the TEM and $CH4MOD_{wetland}$ (Table 3).

The two models simulated similar spatial distributions of the CH_4 emissions among different wetland types and continents (Table 3). Marshes emit higher CH_4 fluxes and have the largest area. Thus, marshes were the greatest contributor to global CH_4 emissions and contributed 36%–39% to global CH_4 emissions (Table 3). Lakes/rivers and swamps were the second and third contributors, respectively (Table 3). The CH_4 emissions from peatlands, coastal wetlands, intermittent wetlands and no-specific wetlands accounted for only approximately 20% of the global emissions (Table 3).

Although North America accounted for 36% of the global wetland area, it contributed only 22%–23% to global emissions (Table 3). In contrast, the wetland area in South America accounted for 15% of the global area and contributed 25%–26% to global CH_4 emissions. Asia and Africa also accounted for approximately 20% of global emissions. The lowest area and emissions were found in Oceania (Table 3).

3.2.3 Global CH_4 estimations

The global CH_4 emissions for the period 2000-2010 were estimated to be 105.31± 2.72 Tg yr^{-1} by Method A and 134.31 ± 0.84 Tg yr^{-1} by Method B. Based on the evaluation of model performance (Table 2), $CH4MOD_{wetland}$ yielded the most accurate predictions for Asia and Europe, and the TEM yielded the most accurate predictions for North America and South America/Africa. Using this combination, the global CH_4 emissions were estimated to be 124.74 ± 1.22 Tg by Method C. Similarly, in Method D, $CH4MOD_{wetland}$ was used for simulations in marshes and coastal wetlands, and the TEM was used for simulations in peatlands and swamps; as a result, the global wetland CH_4 emissions were estimated to be 116.99 ± 2.23 Tg.

4. Discussion

4.1 Generality of $CH4MOD_{wetland}$ and the TEM

A lack of correspondence between the model output and observations could be partly due to the observed flux data, e.g., the inevitable gap-filling of missing data points to determine the seasonal/annual total emissions (Kramer et al., 2002). The results showed differences between the observed and simulated CH_4 emissions by both $CH4MOD_{wetland}$ and the TEM on a global scale (Fig. 2) and continent scale (Fig. 3) and for different wetland types (Fig. 4). The reliability of the observed flux data was not under discussion in this study. We evaluated only the model accuracy and applicability across different wetland types and continents.

On a global scale, both models fulfilled the criteria of sufficient accuracy for the ability to predict CH_4 fluxes (Table 2). However, this fuzzy analysis may miss some real model performance. For the model applicability on different continents, $CH4MOD_{wetland}$ performed best in Asia, followed by North America and Europe. It performed poorly in South America/Africa, where swamps are more common (Table 2). The TEM performed best in North America, followed by South America/Africa and Asia. It performed poorly in Europe (Table 2). Each continent has different main wetland types; thus, the model applicability for different continents depended on its applicability for different types. $CH4MOD_{wetland}$ is suitable for marshes, peatlands and coastal wetlands, but it cannot be applied in swamps (Table 2). This limitation may be because in $CH4MOD_{wetland}$, only a semiempirical logistic model is used to simulate plant growth (Li et al., 2010). This characteristic may induce large uncertainties in simulating the growth of forests in swamps (Table 1). However, the TEM uses the carbon nitrogen dynamics module (CNDM) to describe the effects of photosynthesis, respiration, decomposition and nutrient cycling on NPP (Melillo et al., 1993). Compared with $CH4MOD_{wetland}$, the TEM performed well in simulating NPP in various vegetation types (Melillo et al., 1993). According to the model evaluation, the TEM was suitable for swamps and peatlands but had large uncertainties in marshes and coastal wetlands (Table 2). This pattern may be because the TEM focuses on two major wetland types: boreal tundra and forest wetland (Zhuang et al., 2004). The biochemical processes in the TEM model may be suitable for peatlands (tundra) and swamps (forest wetland) but not suitable for marshes. For coastal wetlands, the TEM did not consider the inhibition of salinity on CH_4 production (Poffenbarger et al., 2011; Bartlett et al., 1987) and greatly overestimated the CH_4 fluxes (Table 2). $CH4MOD_{wetland}$ introduced the influence of salinity on CH_4 production and had good performance for coastal wetlands (Table 2).

4.2 Reducing uncertainties in global estimations

The estimates of global wetland CH_4 emissions had large ranges in previous studies (Zhu et al., 2015). The estimates by process-based models ranged from 92 Tg yr^{-1} (Cao et al., 1996) to 297 Tg yr^{-1} (Gedney et al., 2004) during the period of 1980-2012. Recently, an ensemble of process-based models driven by the same climatic data has commonly been used to estimate global wetland CH_4 emissions (Melton et al., 2013; Kirschke et al., 2013; Poulter et al., 2017; Saunois et al., 2016). However, the uncertainties in the model mean estimation range from 12% (Poulter et al., 2017) to 40% (Melton et al., 2013). The uncertainty mainly comes from the wetland distribution and model structure and parameters (Saunois et al., 2016). Estimating accurate wetland extent and its seasonal and annual variations is a major challenge in present studies. The global estimations of wetland area ranged from 4.3 M ha to 12.9 M ha during the period of 1990 to 2005 (Melton et al., 2013). The wetland extent of 9.2 M ha from the GLWD excluded water bodies, and this value was ~40% higher than the wetland area used in this study. That is, this difference was the main reason for the lower global estimations determined in this study than those reported in previous works (Zhu et al., 2015; Melton et al., 2013; Poulter et al., 2017; Saunois et al., 2016). Improving the accuracy of wetland extent and temporal variations is important in reducing uncertainties in global wetland CH_4 estimations.

In addition to wetland area, the model structure and parameters accounted for ~70% of the total uncertainties (Saunois et al., 2016). The results of the accuracy analysis showed that for $CH4MOD_{wetland}$, regression bias accounted for 61% of the model errors in peatland, and mean bias accounted for 22% of the RMSE in swamp; for the TEM, mean bias and regression bias accounted for 29% and 42%, respectively, of the model errors in coastal wetland (Table 2). This result indicated that there were still uncertainties in the modeling procedure, e.g., in the model mechanism or in parameterization (Zhang et al., 2017; Allen and Raktoe, 1981). In the existing process-based models, which are not limited to $CH4MOD_{wetland}$ and the TEM, some important procedures should be focused on to reduce the bias due to the model mechanism. For example, the mechanism of the freeze-thaw cycle is important in process-based models (Wei and Wang, 2017) because of the large contribution of CH_4 released during the nongrowing season in some frozen regions (Friborg et al., 1997; Huttunen et al., 2003; Mastepanov et al., 2008; Zona et al., 2016). In addition, quantifying CH_4 ebullition is important but difficult due to the uncertainty in estimates of CH_4 emissions from peatlands (Stanley et al., 2019). Moreover, although the importance of plants in CH_4 biogeochemical processes has been reported in many studies, better modeling and characterization of plant community structure is needed (Bridgham et al., 2013). Finally, most of the present process-based models do not have the ability to simulate CH_4 exchange from water bodies, such as lakes, rivers and reservoirs, although such water bodies contribute significantly to the global budget (Deemer et al., 2016). The use of the IPCC Tier method inevitably induces large uncertainties in the global estimates. The above mechanisms should be incorporated into existing process-based models to reduce the uncertainties in the current assessment.

The observational data related to processes of and controls on CH_4 production, consumption, and transport also limit the model calibration and validation. The flux data of 43 wetland sites used for model performance in this study are quite limited and do not represent all climatic, soil, hydrologic and vegetation conditions across global natural wetlands (Table 1). The observations in this study used both the chamber method and the eddy covariance method (Aubinet et al., 2012), which are widely used for CH_4 observations (Table 1). There are differences in measuring CH_4 fluxes between the two methods (Chaichana et al., 2018). The eddy covariance method may underestimate the fluxes (Twine et al., 2000; Sachs et al., 2010), while the chamber method may overestimate the fluxes (Werle and Kormann, 2001). These differences may introduce uncertainties to model calibration and validation. Furthermore, both process-based models were evaluated on an annual basis rather than on a daily scale. The validation of seasonal variation was not performed in this study, partly because we cannot obtain the daily step data for some of the sites. Fine temporal validation against more flux datasets, especially fluxes by eddy covariance experiments, and intermediate variables that control the CH_4 process are necessary in future studies (Wei and Wang, 2017).

5. Conclusion

Two process-based models, $CH4MOD_{wetland}$ and the TEM, were used to simulate annual CH_4 emissions from different wetland types and continents, and their performances were evaluated. Model validation showed that both models could simulate variations between different wetland sites and years.

The statistical analysis of model performance showed that $CH4MOD_{wetland}$ was capable of simulating CH_4 emissions from marshes, peatlands, swamps and coastal wetlands, while the TEM was capable of simulating CH_4 emissions from peatlands and swamps (model efficiency > 0). $CH4MOD_{wetland}$ performed well in Asia, Europe and North America, while the TEM performed well in North America, Asia, South America and Africa. The models were then used to estimate global wetland CH_4 emissions. The CH_4 simulations of both models had good agreement in terms of the latitudinal and meridional bands. The global CH_4 emissions for the period 2000–2010 were estimated to be 105.31± 2.72 Tg yr^{-1} by $CH4MOD_{wetland}$ and 134.31 ± 0.84 Tg yr^{-1} by the TEM. If we used a more accurate model to estimate each continent/wetland type based on the models' generality, the estimated global CH_4 emissions were 116.99–124.74 Tg yr^{-1} for the period 2000–2010. The uncertainty in global wetland CH_4 assessments by the process-based model approach comes from the inaccuracy of the wetland mapping area, the modeling procedure and the observational limitations. Future research on accurately mapping wetlands, improving model mechanisms and parametrization and using more observations to evaluate model performance would improve global estimations.

Code and data availability.

The TEM and $CH4MOD_{wetland}$ model code and model data sets (input data and model results) are available on the website https://zenodo.org/record/3594988#.XglabvkzY2w.

Author Contribution

T. Li and L. Yu pondered the rationale of the method. T. Li and Y. Lu developed and performed the model simulations. W. Sun, Q. Zhang, W. Zhang, G. Wang, Z. Qin, L. Yu, H. Li and R. Zhang made the data collection and processing. T. Li prepared the manuscript with contributions from all coauthors.

Acknowledgments.

This work was jointly supported by the National Natural Science Foundation of China (Grant No. 91937302, 41775159, 31000234 and 41075107).

Competing Interests

The authors declare no competing interests.

References

Allen, O. B., and Raktoe, B. L.: Accuracy analysis with special reference to the prediction of grassland yield, Biom. J., 23, 371-388, 1981.

Alvalá, P. C., and Kirchhoff, V. W. J. H.: Methane fluxes from the Pantanal floodplain in Brazil: seasonal variation, in: Non-CO_2 greenhouse gases: Scientific understanding, control and implementation: Proceedings of the Second International Symposium, Noordwijkerhout, The Netherlands, 8–10 September 1999, edited by: van Ham, J., Baede, A. P. M., Meyer, L. A., and Ybema, R., Springer Netherlands, Dordrecht, 95-99, 2000.Antonov, J. I., Seidov, D., Boyer, T. P., Locarnini, R. A., Mishonov, A. V., Garcia, H. E., Baranova, O. K., Zweng, M. M., and Johnson, D. R.: World Ocean Atlas 2009Volume 2: Salinity. , in: NOAA Atlas NESDIS 69, edited by: Levitus, S., U.S. Government Printing Office,, 2010.

Aubinet, M., Vesala, T., and Papale, D.: Eddy covariance: a practical guide to measurement and data analysis, Springer Science & Business Media, 2012.

Aurela, M., Laurila, T., and Tuovinen, J. P.: Annual CO_2 balance of a subarctic fen in northern Europe: importance of the wintertime efflux, J. Geophys. Res.: Atmos., 107, 4607, 10.1029/2002JD002055, 2002.

Bartlett, K., Harriss, R., and Sebacher, D.: Methane flux from coastal salt marshes, J. Geophys. Res. Atmos., 90(D3), 5710-5720, 1985.

Bartlett, K., Crill, P., Sass, R., Harriss, R., and Dise, N.: Methane emissions from tundra environments in the Yukon-Kuskokwim Delta, Alaska, J. Geophys. Res., 97(D15), 16645-16660, 10.1029/91JD00610, 1992.

Bartlett, K. B., Bartlett, D. S., Harriss, R. C., and Sebacher, D. I.: Methane emissions along a salt marsh salinity gradient, Biogeochemistry, 4, 183-202, 10.1007/bf02187365, 1987.

Belward, A. S., Estes, J. E., and Kline, K. D.: The IGBP-DIS global 1-km land-cover data set DISCover: A project overview, Photogramm. Eng. Remote Sens., 65, 1013-1020, 1999.

Belger, L., Forsberg, B. R., and Melack, J. M.: Carbon dioxide and methane emissions from interfluvial wetlands in the upper Negro River basin, Brazil, Biogeochemistry, 105, 171-183, 10.1007/s10533-010-9536-0, 2011.

Bennett, N. D., Croke, B. F. W., Guariso, G., Guillaume, J. H. A., Hamilton, S. H., Jakeman, A. J., Marsili-Libelli, S., Newham, L. T. H., Norton, J. P., Perrin, C., Pierce, S. A., Robson, B., Seppelt, R., Voinov, A. A., Fath, B. D., and Andreassian, V.: Characterising performance of environmental models, Environ. Model. Software, 40, 1-20, https://doi.org/10.1016/j.envsoft.2012.09.011, 2013.

Beven, K., and Kirkby, M. J.: A physically based, variable contributing area model of basin hydrology, Hydrol. Sci. Bull., 24, 43-69, 1979.

Bhullar, G. S., Iravani, M., Edwards, P. J., and Venterink, H. O.: Methane transport and emissions from soil as affected by water table and vascular plants, BMC Ecol., 13, 32, 2013.

Bohn, T., Lettenmaier, D., Sathulur, K., Bowling, L., Podest, E., McDonald, K., and Friborg, T.: Methane emissions from western Siberian wetlands: heterogeneity and sensitivity to climate change, Environ. Res. Lett., 2, 045015, doi:10.1088/1748-9326/2/4/045015, 2007.

Bousquet, P., Ciais, P., Miller, J., Dlugokencky, E., Hauglustaine, D., Prigent, C., Van der Werf, G., Peylin, P., Brunke, E.-G., and Carouge, C.: Contribution of anthropogenic and natural sources to atmospheric methane variability, Nature, 443, 439-443, 2006.

Boucher, O., Friedlingstein, P., Collins, B., and Shine, K. P.: The indirect global warming potential and global temperature change potential due to methane oxidation, Environ. Res. Lett., 4, 044007, 10.1088/1748-9326/4/4/044007, 2009.

Bridgham, S., Updegraff, K., and Pastor, J.: Carbon, Nitrogen, and Phosphorus Mineralization in Northern Wetlands, Ecology, 79, 1545-1561, 1998.

Bridgham, S. D., Cadillo-Quiroz, H., Keller, J. K., and Zhuang, Q.: Methane emissions from wetlands: biogeochemical, microbial, and modeling perspectives from local to global scales, Global Change Biol., 19, 1325-1346, 2013.

Bruhwiler, L., Dlugokencky, E., Masarie, K., Ishizawa, M., Andrews, A., Miller, J., Sweeney, C., Tans, P., and Worthy, D.: Carbon Tracker CH_4: an assimilation system for estimating emissions of atmospheric methane, Atmos. Chem. Phys., 14, 8269-8293, 10.5194/acp-14-8269-2014, 2014.

Cao, M., Marshall, S., and Gregson, K.: Global carbon exchange and methane emissions from natural wetlands: Application of a process-based model, J. Geophys. Res.: Atmos., 101, 14399-14414, 1996.

Carter, A. J., and Scholes, R. J.: Spatial global database of soil properties., IGBP Global Soil Data Task CD-ROM (International Geosphere-Biosphere Programme Data Information Systems. Toulouse, France 2000), 2000.

Chaichana, N., Bellingrath-Kimura, S., Komiya, S., Fujii, Y., Noborio, K., Dietrich, O., and Pakoktom, T.: Comparison of closed chamber and eddy covariance methods to improve the understanding of methane fluxes from rice paddy fields in Japan, Atmosphere, 9, 356, 2018.

Chanton, J. P.: The effect of gas transport on the isotope signature of methane in wetlands, Org. Geochem., 36, 753-768, 2005.

Christensen, T., Friborg, T., Sommerkorn, M., Kaplan, J., Illeris, L., Soegaard, H., Nordstroem, C., and Jonasson, S.: Trace gas exchange in a high-Arctic valley: 1. Variationsin CO_2 and CH_4 flux between tundra vegetation types, Global Biogeochem. Cycles, 14, 701-713, 2000.

Christensen, T. R.: Methane emission from Arctic tundra, Biogeochemistry, 21, 117-139, 10.1007/BF00000874, 1993.

Crill, P. M., Bartlett, K. B., Wilson, J. O., Sebacher, D. I., Harriss, R. C., Melack, J. M., MacIntyre, S., Lesack, L., and Smith-Morrill, L.: Tropospheric methane from an Amazonian floodplain lake, J. Geophys. Res.: Atmos., 93, 1564-1570, 10.1029/JD093iD02p01564, 1988.

Dalsøren, S. B., Myhre, C. L., Myhre, G., Gomez-Pelaez, A. J., Søvde, O. A., Isaksen, I. S. A., Weiss, R. F., and Harth, C. M.: Atmospheric methane evolution the last 40 years, Atmos. Chem. Phys., 16, 3099-3126, 10.5194/acp-16-3099-2016, 2016.

Deemer, B. R., Harrison, J. A., Li, S., Beaulieu, J. J., DelSontro, T., Barros, N., Bezerra-Neto, J. F., Powers, S. M., dos Santos, M. A., and Vonk, J. A.: Greenhouse gas emissions from reservoir water surfaces: A new global synthesis, BioScience, 66, 949-964, 10.1093/biosci/biw117, 2016.

Delaune, R., Smith, C., Patrick, W., and Jr, W.: Methane release from Gulf coast wetlands, Tellus B, 35B, 8-15, 10.1111/j.1600-0889.1983.tb00002.x, 1983.

Devol, A. H., Richey, J. E., Clark, W. A., King, S. L., and Martinelli, L. A.: Methane emissions to the troposphere from the Amazon floodplain, J. Geophys. Res.: Atmos., 93, 1583-1592, 10.1029/JD093iD02p01583, 1988.

Dlugokencky, E., Bruhwiler, L., White, J., Emmons, L., Novelli, P. C., Montzka, S. A., Masarie, K. A., Lang, P. M., Crotwell, A., and Miller, J. B.: Observational constraints on recent increases in the atmospheric CH_4 burden, Geophys. Res. Lett., 36, 2009.

Dlugokencky, E. J.: NOAA/ESRL (www.esrl.noaa.gov/gmd/ccgg/trends_ch4/)(Accessed: 18 July 2016), 2016.

Duan, X., Wang, X., Mu, Y., and Ouyang, Z.: Seasonal and diurnal variations in methane emissions from

Wuliangsu Lake in arid regions of China, Atmos. Environ., 39, 4479-4487, 2005.
Fan, Y., and van den Dool, H.: Climate Prediction Center global monthly soil moisture data set at 0.5 resolution for 1948 to present, J. Geophys. Res.: Atmos., 109, D10102, doi:10.1029/2003JD004345, 2004.
Fan, S. M., Wofsy, S. C., Bakwin, P. S., Jacob, D. J., Anderson, S. M., Kebabian, P. L., McManus, J. B., Kolb, C. E., and Fitzjarrald, D. R.: Micrometeorological measurements of CH_4 and CO_2 exchange between the atmosphere and subarctic tundra, J. Geophys. Res.: Atmos., 97, 16627-16643, 10.1029/91jd02531, 1992.
FAO/IIASA/ISRIC/ISS-CAS/JRC: Harmonized World Soil Database, version 1.0, FAO, Rome, Italy and IIASA, Laxenburg, Austria, 42pp, 2008.
FAO/IIASA/ISRIC/ISS-CAS/JRC: Harmonized World Soil Database, version 1.2, FAO and IIASA, Rome, Italy and Laxenburg, Austria, 43pp, 2012.
Farr, T. G., Rosen, P. A., Caro, E., Crippen, R., Duren, R., Hensley, S., Kobrick, M., Paller, M., Rodriguez, E., Roth, L., Seal, D., Shaffer, S., Shimada, J., Umland, J., Werner, M., Oskin, M., Burbank, D., and Alsdorf, D.: The shuttle radar topography mission, Rev. Geophys., 45, 10.1029/2005rg000183, 2007.
Fraser, A., Palmer, P., Feng, L., Boesch, H., Cogan, A., Parker, R., Dlugokencky, E., Fraser, P., Krummel, P., and Langenfelds, R.: Estimating regional methane surface fluxes: the relative importance of surface and GOSAT mole fraction measurements, Atmos. Chem. Phys., 13, 5697-5713, doi:10.5194/acp-13-5697-2013, 2013.
Friborg, T., Christensen, T., and Søgaard, H.: Rapid response of greenhouse gas emission to early spring thaw in a subarctic mire as shown by micrometeorological techniques, Geophys. Res. Lett., 24, 3061-3064, doi: 10.1029/97GL03024, 1997.
Galand, P., Yrjälä, K., and R, C.: Stable carbon isotope fractionation during methanogenesis in three boreal peatland ecosystems, Biogeosciences, 7, 5497-5515, 10.5194/bgd-7-5497-2010, 2010.
Gedney, N., Cox, P., and Huntingford, C.: Climate feedback from wetland methane emissions, Geophys. Res. Lett., 31, doi:10.1029/2004GL020919, 2004.
Ghosh, A., Patra, P., Ishijima, K., Umezawa, T., Ito, A., Etheridge, D., Sugawara, S., Kawamura, K., Miller, J., and Dlugokencky, E.: Variations in global methane sources and sinks during 1910–2010, Atmos. Chem. Phys., 15, 2595-2612, 2015.
Hao, Q. J.: Effect of land-use change on greenhouse gases emissions in freshwater marshes in the Sanjiang Plain, Ph.D. Dissertation, Institute of Atmospheric Physics, Chinese Academy of Sciences, Beijing, 2006.
Harris, I., Jones, P., Osborn, T., and Lister, D.: Updated high-resolution grids of monthly climatic observations–the CRU TS3. 10 Dataset, Int. J. Clim., 34, 623-642, 2014.
Hirota, M., Tang, Y., Hu, Q., Hirata, S., Kato, T., Mo, W., Cao, G., and Mariko, S.: Methane emissions from different vegetation zones in a Qinghai-Tibetan Plateau wetland, Soil Biol. Biochem., 36, 737-748, 2004.
Huang, G., Li, X., Hu, Y., Shi, Y., and Xiao, D.: Methane (CH_4) emission from a natural wetland of northern China, J. Environ. Sci. Health, 40, 1227-1238, 2005.
Huang, P. Y., Yu, H. X., Chai, L. H., Chai, F. Y., and Zhang, W. F.: Methane emission flux of Zhalong Phragmites Australis wetlands in growth season., Chin. J. Applied Ecol., 22, 1219-1224, 2011.
Huang, Y., Sass, R. L., and Fisher Jr, F. M.: A semi-empirical model of methane emission from flooded rice paddy soils, Global Change Biol., 4, 247-268, 1998.
Huang, Y. A. O., Sass, R., and Fisher, F.: Methane emission from Texas rice paddy soils. 1. Quantitative

multi-year dependence of CH_4 emission on soil, cultivar and grain yield, Global Change Biol., 3, 479-489, 1997.
Hanis, K., Tenuta, M., Amiro, B., and Papakyriakou, T.: Seasonal dynamics of methane emissions from a subarctic fen in the Hudson Bay Lowlands, Biogeosciences Discuss., 10, 4539-4574, doi:10.5194/bgd-10-4539-2013, 2013.
Harazono, Y., Mano, M., Miyata, A., Yoshimoto, M., Zulueta, R., Vourlitis, G., Kwon, H., and Oechel, W.: Temporal and spatial differences of methane flux at arctic tundra in Alaska, Mem. Natl. Inst. Polar Res., 59, 79-95, 2006.
Hatala, J. A., Detto, M., Sonnentag, O., Deverel, S. J., Verfaillie, J., and Baldocchi, D. D.: Greenhouse gas (CO_2, CH_4, H_2O) fluxes from drained and flooded agricultural peatlands in the Sacramento-San Joaquin Delta, Agric., Ecosyst. Environ., 150, 1-18, 2012.
Huttunen, J. T., Alm, J., Saarijärvi, E., Lappalainen, K. M., Silvola, J., and Martikainen, P. J.: Contribution of winter to the annual CH_4 emission from a eutrophied boreal lake, Chemosphere, 50, 247-250, 2003.
IPCC: Revised 1996 IPCC Guidelines for National Greenhouse Gas Inventories: Reference Manual., 1996.
Jauhiainen, J., Takahashi, H., Heikkinen, J. E., Martikainen, P. J., and Vasander, H.: Carbon fluxes from a tropical peat swamp forest floor., Global Change Biol., 11, 1788-1797, 2005.
Jitka, V., Jiří, D., Stanislav, S., Lenka, M., and Hana, Č.: Effect of hummock-forming vegetation on methane emissions from a temperate sedge-grass marsh, Wetlands, 37, 675-686, 10.1007/s13157-017-0898-0, 2017.
Joabsson, A., and Christensen, T. R.: Methane emissions from wetlands and their relationship with vascular plants: an Arctic example, Global Change Biol., 7, 919-932, doi:10.1046/j.1354-1013.2001.00044.x, 2001.
Kang, W. X., Zhao, Z. H., Tian, D. L., He, J. N., and Deng, X. W.: CO_2 exchanges between mangrove- and shoal wetland ecosystems and atmosphere in Guangzhou, Chin. J. Appl. Ecol., 19, 2605-2610, 2008.
Keddy, P. A.: Wetland ecology: principles and conservation, Cambridge University Press, 2010.
Keller, J., and Bridgham, S.: Pathways of Anaerobic Carbon Cycling Across an Ombrotrophic–Minerotrophic Peatland Gradient, Limnol. Oceanogr., 52, 96-107, 10.4319/lo.2007.52.1.0096, 2007.
King, J., Reeburgh, W., Thieler, K., Kling, G., Loya, W., Johnson, L., and Nadelhoffer, K.: Pulse-labeling studies of carbon cycling in Arctic tundra ecosystems: The contribution of photosynthates to methane emission, Global Biogeochem. Cycles, 16, 2002.
Kingsford, R. T., Basset, A., and Jackson, L.: Wetlands: conservation's poor cousins, Aquatic Conservation: Marine and Freshwater Ecosystems, 26, 892-916, 10.1002/aqc.2709, 2016.
Kirschke, S., Bousquet, P., Ciais, P., Saunois, M., Canadell, J. G., Dlugokencky, E. J., Bergamaschi, P., Bergmann, D., Blake, D. R., and Bruhwiler, L.: Three decades of global methane sources and sinks, Nat. Geosci., 6, 813-823, 2013.
Koh, H. S., Ochs, C., and Yu, K.: Hydrologic gradient and vegetation controls on CH_4 and CO_2 fluxes in a spring-fed forested wetland, Hydrobiologia, 630, 271-286, 10.1007/s10750-009-9821-x, 2009.
Kramer, K., Leinonen, I., Bartelink, H., Berbigier, P., Borghetti, M., Bernhofer, C., Cienciala, E., Dolman, A., Froer, O., and Gracia, C.: Evaluation of six process-based forest growth models using eddy-covariance measurements of CO_2 and H_2O fluxes at six forest sites in Europe, Global Change Biol., 8, 213-230, 2002.
Kwon, M. J., Beulig, F., Ilie, I., Wildner, M., Küsel, K., Merbold, L., Mahecha, M. D., Zimov, N., Zimov,

S. A., Heimann, M., Schuur, E. A. G., Kostka, J. E., Kolle, O., Hilke, I., and Göckede, M.: Plants, microorganisms, and soil temperatures contribute to a decrease in methane fluxes on a drained Arctic floodplain, Global Change Biol., 23, 2396-2412, 10.1111/gcb.13558, 2017.

Lehner, B., and Döll, P.: Development and validation of a global database of lakes, reservoirs and wetlands, Journal of Hydrology, 296, 1-22, 2004.

Li, T., Huang, Y., Zhang, W., and Song, C.: $CH4MOD_{wetland}$: A biogeophysical model for simulating methane emissions from natural wetlands, Ecol. Model., 221, 666-680, 2010.

Li, T., Zhang, W., Zhang, Q., Lu, Y., Wang, G., Niu, Z., Raivonen, M., and Vesala, T.: Impacts of climate and reclamation on temporal variations in CH_4 emissions from different wetlands in China: from 1950 to 2010, Biogeosciences, 12, 6853-6868, 10.5194/bg-12-6853-2015, 2015.

Li, T., Xie, B., Wang, G., Zhang, W., Zhang, Q., Vesala, T., and Raivonen, M.: Field-scale simulation of methane emissions from coastal wetlands in China using an improved version of $CH4MOD_{wetland}$, Sci. Total Environ., 559, 256-267, http://dx.doi.org/10.1016/j.scitotenv.2016.03.186, 2016.

Li, T., Zhang, Q., Cheng, Z., Wang, G., Yu, L., and Zhang, W.: Performance of $CH4MOD_{wetland}$ for the case study of different regions of natural Chinese wetland, J. Environ. Sci., 57, 356-369, 2017.

Li, T., Li, H., Zhang, Q., Ma, Z., Yu, L., Lu, Y., Niu, Z., Sun, W., and Liu, J.: Prediction of CH_4 emissions from potential natural wetlands on the Tibetan Plateau during the 21st century, Sci. Total Environ., 657, 498-508, https://doi.org/10.1016/j.scitotenv.2018.11.275, 2019.

Li, Y. J., Cheng, Z. L., Wang, D. Q., Hu, H., and Wang, C.: Methane emission in the process of wetland and vegetation succession in salt marsh of Yangtze River estuary, Acta Sci. Circumst., 34 2035-2402, 2014.

Loveland, T., Reed, B., Brown, J., Ohlen, D., Zhu, Z., Yang, L., and Merchant, J.: Development of a global land cover characteristics database and IGBP DISCover from 1 km AVHRR data, Int. J. Remote Sens., 21, 1303-1330, 2000.

Marthews, T., Dadson, S., Lehner, B., Abele, S., and Gedney, N.: High-resolution global topographic index values for use in large-scale hydrological modelling, Hydrol. Earth Syst. Sci., 19, 91-104, 2015.

Mastepanov, M., Sigsgaard, C., Dlugokencky, E. J., Houweling, S., Ström, L., Tamstorf, M. P., and Christensen, T. R.: Large tundra methane burst during onset of freezing, Nature, 456, 628-630, 2008.

McEwing, K. R., Fisher, J. P., and Zona, D.: Environmental and vegetation controls on the spatial variability of CH4 emission from wet-sedge and tussock tundra ecosystems in the Arctic, Plant Soil, 388, 37-52, 10.1007/s11104-014-2377-1, 2015.

Meirink, J. F., Bergamaschi, P., and Krol, M. C.: Four-dimensional variational data assimilation for inverse modelling of atmospheric methane emissions: method and comparison with synthesis inversion, Atmos. Chemis. Phys., 8, 6341-6353, 2008.

Melack, J. M., Hess, L. L., Gastil, M., Forsberg, B. R., Hamilton, S. K., Lima, I. B. T., and Novo, E. M. L. M.: Regionalization of methane emissions in the Amazon Basin with microwave remote sensing, Global Change Biol., 10, 530-544, 10.1111/j.1365-2486.2004.00763.x, 2004.

Melillo, J. M., McGuire, A. D., Kicklighter, D. W., Moore, B., Vorosmarty, C. J., and Schloss, A. L.: Global climate change and terrestrial net primary production, Nature, 363, 234-240, 1993.

Melling, L., Hatanoa, R., and Gohc, K. J.: Methane fluxes from three ecosystems in tropical peatland of Sarawak, Malaysia, Soil Biol. Biochem., 37, 1445-1453, 2005.

Melton, J., Wania, R., Hodson, E., Poulter, B., Ringeval, B., Spahni, R., Bohn, T., Avis, C., Beerling, D., and Chen, G.: Present state of global wetland extent and wetland methane modelling: conclusions from a model intercomparison project (WETCHIMP), Biogeosciences, 10, 753-788, 2013.

Meng, L., Hess, P. G. M., Mahowald, N. M., Yavitt, J. B., Riley, W. J., Subin, Z. M., Lawrence, D. M., Swenson, S. C., Jauhiainen, J., and Fuka, D. R.: Sensitivity of wetland methane emissions to model assumptions: application and model testing against site observations, Biogeosciences, 9, 2793-2819, 10.5194/bg-9-2793-2012, 2012.

Moore, T., Roulet, N., and Knowles, R.: Spatial and temporal variations of methane flux from subarctic/northern Boreal fens, Global Biogeochem. Cycles, 4, 29-46, 10.1029/GB004i001p00029, 1990.

Moore, T., Heyes, A., and Roulet, N.: Methane emissions from wetlands, southern Hudson Bay Lowland, J. Geophys. Res., 99, 10.1029/93JD02457, 1994.

Moore, T., Young, A., Bubier, J., Humphreys, E., Lafleur, P., and Roulet, N.: A multi-year record of methane flux at the Mer Bleue Bog, Southern Canada, Ecosystems, 14, 646-657, 10.1007/s10021-011-9435-9, 2011.

Morse, J. L., Ardón, M., and Bernhardt, E. S.: Greenhouse gas fluxes in southeastern U.S. coastal plain wetlands under contrasting land uses, Ecol. Appl., 22, 264-280, 10.1890/11-0527.1, 2012.

Myhre, G., Shindell, D., Bréon, F. M., Collins, W., Fuglestvedt, J., Huang, J., Koch, D., Lamarque, J. F., Lee, D., Mendoza, B., Nakajima, T., Robock, A., Stephens, G., Takemura, T., and Zhang, H.: Anthropogenic and Natural Radiative Forcing, in: In Climate Change 2013: The Physical Science Basis. Contribution of Working Group I to the Fifth Assessment Report of the Inter-governmental Panel on Climate Change, edited by: Stocker, T. F., Qin, D., Plattner, G. K., Tignor, M., Allen, S. K., Boschung, J., Nauels, A., Xia, Y., Bex, V., and Midgley, P. M., Cambridge University Press, Cambridge, UK and New York, NY, USA, 2013.

Long, K. D., Flanagan, L. B., and Cai, T.: Diurnal and seasonal variation in methane emissions in a northern Canadian peatland measured by eddy covariance, Global Change Biol., 16, 2420-2435, 10.1111/j.1365-2486.2009.02083.x, 2010.

Nakano, T., Kuniyoshi, S., and Fukuda, M.: Temporal variation in methane emission from tundra wetlands in a permafrost area, northeastern Siberia, Atmos. Environ., 34, 1205-1213, 10.1016/S1352-2310(99)00373-8, 2000.

Nisbet, E., Manning, M., Dlugokencky, E., Fisher, R., Lowry, D., Michel, S., Lund Myhre, C., Platt, S., Allen, G., Bousquet, P., Brownlow, R., Cain, M., France, J., Hermansen, O., Hossaini, R., Jones, A., Levin, I., Manning, A., Myhre, G., and White, J.: Very strong atmospheric methane growth in the four years 2014-2017: Implications for the Paris Agreement, Global Biogeochem. Cycles, 10.1029/2018GB006009, 2019.

Olefeldt, D., Roulet, N. T., Bergeron, O., Crill, P., Bäckstrand, K., and Christensen, T. R.: Net carbon accumulation of a high-latitude permafrost palsa mire similar to permafrost-free peatlands, Geophys. Res. Lett., 39, L03501, 10.1029/2011GL050355, 2012.

Olson, D., Griffis, T., Noormets, A., Kolka, R., and Chen, J.: Interannual, seasonal, and retrospective analysis of the methane and carbon dioxide budgets of a temperate peatland, J. Geophys. Res.: Biogeosci., 118, 226-238, 10.1002/jgrg.20031, 2013.

Page, S., Rieley, J., Shotyk, W., and Weiss, D.: Interdependence of peat and vegetation in a tropical peat swamp forest, Philosophical transactions of the Royal Society of London. Series B, Biol. Sci., 354, 1885-1897, 10.1098/rstb.1999.0529, 1999.

Parmentier, F. J. W., van Huissteden, J., van der Molen, M. K., Schaepman-Strub, G., Karsanaev, S. A., Maximov, T. C., and Dolman, A. J.: Spatial and temporal dynamics in eddy covariance observations of methane fluxes at a tundra site in northeastern Siberia, J. Geophys. Res.: Biogeosci., 116, 10.1029/2010jg001637, 2011.

Poffenbarger, H. J., Needelman, B. A., and Megonigal, J. P.: Salinity influence on methane emissions from tidal marshes, Wetlands, 31, 831-842, 10.1007/s13157-011-0197-0, 2011.
Poulter, B., Bousquet, P., Canadell, J. G., Ciais, P., Peregon, A., Saunois, M., Arora, V. K., Beerling, D. J., Brovkin, V., and Jones, C. D.: Global wetland contribution to 2000–2012 atmospheric methane growth rate dynamics, Environ. Res. Lett., 12, 094013, 2017.
Riley, W. J., Subin, Z. M., Lawrence, D. M., Swenson, S. C., Torn, M. S., Meng, L., Mahowald, N. M., and Hess, P.: Barriers to predicting changes in global terrestrial methane fluxes: analyses using CLM4Me, a methane biogeochemistry model integrated in CESM, Biogeosciences, 8, 1925-1953, 10.5194/bg-8-1925-2011, 2011.
Rykiel, E. J.: Testing ecological models: the meaning of validation, Ecol. Model., 90, 229-244, https://doi.org/10.1016/0304-3800(95)00152-2, 1996.
Sachs, T., Giebels, M., Boike, J., and Kutzbach, L.: Environmental controls on CH_4 emission from polygonal tundra on the microsite scale in the Lena river delta, Siberia, Global Change Biol., 16, 3096-3110, 2010.
Saunois, M., Bousquet, P., Poulter, B., Peregon, A., Ciais, P., Canadell, J. G., Dlugokencky, E. J., Etiope, G., Bastviken, D., Houweling, S., Janssens-Maenhout, G., Tubiello, F. N., Castaldi, S., Jackson, R. B., Alexe, M., Arora, V. K., Beerling, D. J., Bergamaschi, P., Blake, D. R., Brailsford, G., Brovkin, V., Bruhwiler, L., Crevoisier, C., Crill, P., Covey, K., Curry, C., Frankenberg, C., Gedney, N., Höglund-Isaksson, L., Ishizawa, M., Ito, A., Joos, F., Kim, H. S., Kleinen, T., Krummel, P., Lamarque, J. F., Langenfelds, R., Locatelli, R., Machida, T., Maksyutov, S., McDonald, K. C., Marshall, J., Melton, J. R., Morino, I., Naik, V., O'Doherty, S., Parmentier, F. J. W., Patra, P. K., Peng, C., Peng, S., Peters, G. P., Pison, I., Prigent, C., Prinn, R., Ramonet, M., Riley, W. J., Saito, M., Santini, M., Schroeder, R., Simpson, I. J., Spahni, R., Steele, P., Takizawa, A., Thornton, B. F., Tian, H., Tohjima, Y., Viovy, N., Voulgarakis, A., van Weele, M., van der Werf, G. R., Weiss, R., Wiedinmyer, C., Wilton, D. J., Wiltshire, A., Worthy, D., Wunch, D., Xu, X., Yoshida, Y., Zhang, B., Zhang, Z., and Zhu, Q.: The global methane budget 2000–2012, Earth Syst. Sci. Data, 8, 697-751, 10.5194/essd-8-697-2016, 2016.
Schimel, J., Nadelhoffer, K., Shaver, G., Giblin, A., Rastetter, E.: Methane and carbon dioxide emissions were monitored in control, greenhouse, and nitrogen and phosphorus fertilized plots of three different plant communities Arctic LTER experimental plots, Toolik Field Station, 1992. Environmental Data Initiative, 1994. http://dx.doi.org/10.6073/pasta/3e2ae7928b00f7546338086d0dc3bd55.
Schimel, J., Nadelhoffer, K., Shaver, G., Giblin, A., Rastetter, E.: Methane and carbon dioxide emissions were monitored in control, greenhouse, and nitrogen and phosphorus fertilized plots of three different plant communities, Toolik Field Station, North Slope Alaska, Arctic LTER 1993. Environmental Data Initiative, 1995. http://dx.doi.org/10.6073/pasta/64c4ad25b7efb6f98acc22301dd1802a.
Sebacher, D., Harriss, R., Bartlett, K., Sebacher, S., and Grice, S.: Atmospheric methane sources: Alaskan tundra bogs, an alpine fen, and a subarctic boreal marsh, Tellus B, 38B, 1-10, 10.1111/j.1600-0889.1986.tb00083.x, 1986.
Shannon, R. D., White, J. R., Lawson, J. E., and Gilmour, B. S.: Methane efflux from emergent vegetation in peatlands, J. Ecology, 239-246, 1996.
Shindell, D., Kuylenstierna, J. C. I., Vignati, E., van Dingenen, R., Amann, M., Klimont, Z., Anenberg, S. C., Muller, N., Janssens-Maenhout, G., Raes, F., Schwartz, J., Faluvegi, G., Pozzoli, L., Kupiainen, K., Höglund-Isaksson, L., Emberson, L., Streets, D., Ramanathan, V., Hicks, K., Oanh, N. T. K., Milly, G., Williams, M., Demkine, V., and Fowler, D.: Simultaneously Mitigating Near-Term Climate Change and Improving Human Health and Food Security, Science, 335, 183, 10.1126/science.1210026, 2012.

Sellers, P. J., Hall, F. G., Kelly, R. D., Black, A., Baldocchi, D., Berry, J., Ryan, M., Ranson, K. J., Crill, P. M., and Lettenmaier, D. P.: BOREAS in 1997: Experiment overview, scientific results, and future directions, J. Geophys. Res.: Atmos., 102, 28731-28769, 1997.

Song, C., Zhang, J., Wang, Y., Wang, Y., and Zhao, Z.: Emission of CO2, CH4 and N2O from freshwater marsh in northeast of China, J. Environ. Manag., 88, 428-436, https://doi.org/10.1016/j.jenvman.2007.03.030, 2008.

Spiers, A. G.: Review of international/continental wetland resources, in: Global review of wetland resources and priorities for wetland inventory, edited by: Finlayson, C. M., and Spiers, A. G., Supervising Scientist Report 144, Supervising Scientist, Canberra, 63 ~ 104, 1999.

Stanley, K. M., Heppell, C. M., Belyea, L. R., Baird, A. J., and Field, R. H.: The Importance of CH_4 Ebullition in Floodplain Fens, J. Geophys. Res.: Biogeosci., 124, 1750-1763, 10.1029/2018jg004902, 2019.

Suyker, A. E., Verma, S. B., Clement, R. J., and Billesbach, D. P.: Methane flux in a boreal fen: Season-long measurement by eddy correlation, J. Geophys. Res.: Atmos., 101, 28637-28647, 1996. doi: 10.1029/96JD02751.Svensson, B., and Rosswall, T.: In situ methane production from acid peat in plant communities with different moisture regimes in a subarctic mire, Oikos, 43, 341, 10.2307/3544151, 1984.

Tathy, J., Cros, B., Delmas, R., Marenco, A., Servant, J., and Labat, M.: CH_4 emission from flooded forest in Central Africa, J. Geophys. Res., 97, 6159-6168, 10.1029/90JD02555, 1992.

Tian, H., Chen, G., Lu, C., Xu, X., Ren, W., Zhang, B., Banger, K., Tao, B., Pan, S., and Liu, M.: Global methane and nitrous oxide emissions from terrestrial ecosystems due to multiple environmental changes, Ecosystem Health and Sustainability, 1(1):4. http://dx.doi.org/10.1890/EHS14-0015.1, 2015.

Tsuruta, A., Aalto, T., Backman, L., Hakkarainen, J., van der Laan-Luijkx, I. T., Krol, M. C., Spahni, R., Houweling, S., Laine, M., Dlugokencky, E., Gomez-Pelaez, A. J., van der Schoot, M., Langenfelds, R., Ellul, R., Arduini, J., Apadula, F., Gerbig, C., Feist, D. G., Kivi, R., Yoshida, Y., and Peters, W.: Global methane emission estimates for 2000–2012 from CarbonTracker Europe-CH4 v1.0, Geosci. Model Dev., 10, 1261-1289, 10.5194/gmd-10-1261-2017, 2017.

Twine, T. E., Kustas, W., Norman, J., Cook, D., Houser, P., Meyers, T., Prueger, J., Starks, P., and Wesely, M.: Correcting eddy-covariance flux underestimates over a grassland, Agricultural and Forest Meteorology, 103, 279-300, 2000.

Wagner, D., Kobabe, S., Pfeiffer, E. M., and Hubberten, H. W.: Microbial controls on methane fluxes from a polygonal tundra of the Lena Delta, Siberia, Permafrost Periglac., 14, 173-185, 2003.

Walter, B. P., and Heimann, M.: A process-based, climate-sensitive model to derive methane emissions from natural wetlands: Application to five wetland sites, sensitivity to model parameters, and climate, Global Biogeochem. Cycles, 14, 745-765, 2000.

Wang, D., Lv, X., Ding, W., Cai, Z., Gao, J., and Yang, F.: Methan emission from narshes in Zoige Plateau, Adv. Earth Sci., 17, 877-880, 2002.

Wei, D., and Wang, X.: Uncertainty and dynamics of natural wetland CH4 release in China: Research status and priorities, Atmos. Environ., 154, 95-105, https://doi.org/10.1016/j.atmosenv.2017.01.038, 2017.

Werle, P., and Kormann, R.: Fast chemical sensor for eddy-correlation measurements of methane emissions from rice paddy fields, Applied Optics, 40, 846-858, 2001.

Whalen, S. C., and Reeburgh, W. S.: Interannual variations in tundra methane emission: A 4-year time series at fixed sites, Global Biogeochem. Cycles, 6, 139-159, 1992.

Wille, C., Kutzbach, L., Sachs, T., Wagner, D., and Pfeiffer, E. M.: Methane emission from Siberian arctic polygonal tundra: eddy covariance measurements and modeling, Global Change Biol., 14, 1395-1408, 2008.

Ye, Y., Lu, C., and Lin, P.: CH_4 dynamics in sediments of Bruguiera sexangula mangrove at Hegang Estuary, Soil Environ. Sci. (in Chinese), 9, 91-95, 2000.

Zhang, Q., Zhang, W., Li, T., Sun, W., Yu, Y., and Wang, G.: Projective analysis of staple food crop productivity in adaptation to future climate change in China, Int. J. Biometeorol., 1-16, 10.1007/s00484-017-1322-4, 2017.

Zhang, Y., Li, C., Trettin, C. C., and Li, H.: An integrated model of soil, hydrology, and vegetation for carbon dynamics in wetland ecosystems, Global Biogeochem. Cycles, 16, 1061-1078, 2002.

Zhu, Q., Liu, J., Peng, C., Chen, H., Fang, X., Jiang, H., Yang, G., Zhu, D., Wang, W., and Zhou, X.: Modelling methane emissions from natural wetlands by development and application of the TRIPLEX-GHG model, Geosci. Model Develop., 7, 981-999, 2014.

Zhu, Q., Peng, C. H., Chen, H., Fang, X. Q., Liu, J. X., Jiang, H., Yang, Y. Z., and Yang, G.: Estimating global natural wetland methane emissions using process modelling: spatio-temporal patterns and contributions to atmospheric methane fluctuations, Global Ecol. Biogeogr., 24, 959-972, 10.1111/geb.12307, 2015.

Zhu, X., Zhuang, Q., Gao, X., Sokolov, A., and Schlosser, C. A.: Pan-Arctic land–atmospheric fluxes of methane and carbon dioxide in response to climate change over the 21st century, Environ. Res. Lett., 8, 045003, doi:10.1088/1748-9326/8/4/045003, 2013.

Zhuang, Q., Melillo, J. M., Kicklighter, D. W., Prinn, R. G., McGuire, A. D., Steudler, P. A., Felzer, B. S., and Hu, S.: Methane fluxes between terrestrial ecosystems and the atmosphere at northern high latitudes during the past century: A retrospective analysis with a process-based biogeochemistry model, Global Biogeochem. Cycles, 18, GB3010, 10.1029/2004gb002239, 2004.

Zhuang, Q., Melillo, J. M., Sarofim, M. C., Kicklighter, D. W., McGuire, A. D., Felzer, B. S., Sokolov, A., Prinn, R. G., Steudler, P. A., and Hu, S.: CO2 and CH4 exchanges between land ecosystems and the atmosphere in northern high latitudes over the 21st century, Geophys. Res. Lett., 33, L17403, doi:10.1029/2006GL026972, 2006.

Zhuang, Q., Melillo, J., McGuire, A., Kicklighter, D., Prinn, R., Steudler, P., Felzer, B., and Hu, S.: Net emissions of CH_4 and CO_2 in Alaska: Implications for the region's greenhouse gas budget, Ecol. Appl., 17, 203-212, 2007.

Zhuang, Q., Chen, M., Xu, K., Tang, J., Saikawa, E., Lu, Y., Melillo, J. M., Prinn, R. G., and McGuire, A. D.: Response of global soil consumption of atmospheric methane to changes in atmospheric climate and nitrogen deposition, Global Biogeochem. Cycles, 27, 650-663, 2013.

Zona, D., Oechel, W., Kochendorfer, J., Paw U, K., Salyuk, A., Olivas, P., Oberbauer, S., and Lipson, D.: Methane fluxes during the initiation of a large-scale water table manipulation experiment in the Alaskan Arctic tundra, Global Biogeochem. Cycles, 23, GB2013, 10.1029/2009GB003487, 2009.

Zona, D., Gioli, B., Commane, R., Lindaas, J., Wofsy, S. C., Miller, C. E., Dinardo, S. J., Dengel, S., Sweeney, C., Karion, A., Chang, R. Y.-W., Henderson, J. M., Murphy, P. C., Goodrich, J. P., Moreaux, V., Liljedahl, A., Watts, J. D., Kimball, J. S., Lipson, D. A., and Oechel, W. C.: Cold season emissions dominate the Arctic tundra methane budget, Proceedings of the National Academy of Sciences, 113, 40-45, 10.1073/pnas.1516017113, 2016.

Table 1. Description of observation wetland sites

ID	Wetland Name, Continent	Location	Wetland Type	Plant Species	Observation Period	Reference
1	Northeast Siberia, Russia, EU	72º22′N, 126º28′E	Peatland [a]	*Carex* spp., *Limprichtia revolvens, Meesia longiseta*	1999.5–1999.9 2003.7–2004.7 [*]	Wagner et al., 2003 Wille et al., 2008
2	Northeast Siberia, Russia, EU	71º30′N, 130º00′E	Peatland [a]	*Eriophorum*, *Carex* spp., *Sphagnum* spp., Salix spp.	1993.7–1993.8	Nakano et al., 2000
3	Northeast Siberia, Russia, EU	68º30′N, 161º24′E	Peatland [a]	*Larix*, *Alnus* spp., *Betula* spp., *Salix* spp.	1995.7–1995.8	Nakano et al., 2000
4	Northeast Siberia, Russia, EU	70°50′N, 147°29′E	Peatland [a]	*Betula nana, Salix pulchra dwarf shrubs, sedge, Sphagnum*	2008.7–2008.8 [*] 2009.6–2009.8 [*]	Parmentier et al., 2011
5	Zackenberg, Greenland, EU	74º30′N, 21º00′W	Peatland	*Cassiope tetragona, Salix arctica*	1996.6–1996.8 1999.7–1999.8 2000.7–2000.8	Christensen et al., 2000; Joabsson and Christensen, 2001
6	Abisko, Sweden, EU	68º22′N, 19º03′E	Peatland [a]	*Eriophorum angustifolium*, *Carex* spp.	1974.6–1974.9 2008–2009 [*]	Svensson and Rosswall, 1984 Olefeldt et al., 2012
7	Kaamanen, Finland, EU	69°08′N, 27°17′E	Peatland	*Shrubs, Carex spp., moss, etc.*	1998.4–1999.4 [*]	Aurela et al., 2002
8	Sanjiang Plain, China, AS [&]	47º35′N, 133º31′E	Marsh	*Carex lasiocarpa, Deyeuxia angustifolia*	2002.6–2005.11	Hao, 2006; Song et al., 2008
9	Ruoergai Plateau, China, AS	32º47′N, 102º32′E	Peatland	*Carex muliensis, Carex meyeriana*	2001.4–2001.10	Wang et al., 2002
10	Wuliangsu Lake, China, AS [&]	40º47′–41º03′ N, 108º43′–108º57′ E	Marsh	*Phragmites australis*	2003. 4–2003.10	Duan et al., 2005
11	Haibei alpine marsh, China, AS	37º29′N, 101º12′E	Marsh	*Carex allivescers*	2002.7–2002.9	Hirota et al., 2004
12	Zhalong Wetland, China, AS	46º52′N–47º32′N, 123º47′E–124º37′E	Marsh	*Phragmites australis*	2009.5–2009.10	Huang et al., 2011
13	Liao River delta, China, AS	40º40′–41º25′N, 121º35′–122º55′E	Coastal [b]	*Phragmites australis*	1997.4–1997.11	Huang et al., 2005
14	Chongming Island, China, AS [&]	31º15′N, 121º30′E	Coastal [b]	*Scirpus*	2004. 5–2004.12 2011.2–2011.12	Li et al., 2014
15	Guangzhou, China, AS	23º01′N, 113º46′E	Coastal [c]	*Aegiceras corniculatum etc.*	2005.3–2005.12 [*]	Kang et al., 2008
16	Haikou, China, AS	19°51′ N, 110°24′ E	Coastal [c]	*Bruguiera sexangula*	1996.1–1997.12 [*]	Ye et al., 2000
17	Sarawak, Malaysia, AS [&]	2º49′N, 111º51′E	Swamp	Flooded forest[$]	2002.8–2003.7	Melling et al., 2005
18	Kalimantan, Indonesia, AS	2º20′S, 113º55′E	Swamp	*Shorea balangeran*	1994.9–1995.9	Page et al., 1999; Jauhiainen et al., 2005
19	Congo River basin, Congo, AF	4º00′S–0º00′, 14º00′–18º00′E	Swamp	Flooded forest[$]	1988 [*]	Tathy et al., 1992
20	Congo River basin, Congo, AF	0º00′–4º00′N, 14º00′–18º00′E	Swamp	Flooded forest[$]	1988 [*]	Tathy et al., 1992
21	Pantanal, Brazil, SA	19º30′S, 57º00′W	Marsh	*Paspalum repens*	1998.1–1998.12	Alvalá and Kirchhoff, 2000; Melack et al., 2004

22	Lago Calado, Brazil, SA	3º15′S, 60º34′W	Swamp	Flooded forest[$]	1985 [*]	Crill et al., 1988
23	Central Brazilian Amazon, SA	5º00′S–0º00′, 50º00′–70 º00′W	Swamp	Flooded forest[$]	1985 [*]	Devol et al., 1988
24	Negro River basin, Brazil, SA	0°17'S, 63°34'W	Swamp	*Emergent sedge, shrub, palm*	2005.1–2006.1 [*]	Belger et al., 2011
25	Alaska bethel, USA, NA	60º45′N, 161º45′W	Peatland [a]	*Empetrum nigrum, Carex aquatilis, Sphagnum spp.*	1988.7–1988.8	Bartlett et al., 1992;
26	Alaska bethel, USA, NA	61º5′N, 162º1′W	Peatland [a]	*Empetrum nigrum, Carex aquatilis, Sphagnum spp.*	1988.7–1988.8	Fan et al., 1992
27	Alaska Prudhoe Bay, USA, NA	70º30′N, 149º00′W	Peatland [a]	*Sphagnum* spp.	1984 [*]	Sebacher et al., 1986
28	Alaska arboretum, USA, NA	64º52′N, 147º51′W	Peatland [a]	*Eriophorum vaginarum*, *Carex* spp., *Sphagnum* spp.	1987.6–1987.10 1988.6–1988.10 1989.6–1989.10	Whalen and Reeburgh, 1992
29	Saskatchewan, Canada, NA [&]	53°57′N,105°57′W	Peatland	*Buckbean*-*Carex* spp.	1994.5–1994.9 1995.5–1995.10	Suyker et al., 1996; Sellers et al., 1997
30	Michigan, USA, NA	42°27′N, 84°01′W	Peatland	*Scheuchzeria palustris*, *Carex oligosperma*	1991.1–1993.12	Shannon et al., 1996
31	Toolik Lake, USA, NA [&]	68°38′N,149°38′W	Peatland [a]	*Eriophorum*, *Carex* spp.	1990.6–1990.8 1992.6–1992.8 1993.5–1993.9	Christensen, 1993 Schimel et al., 1994, 1995
32	Hudson Bay, Canada, NA	51°18′–51°31′N, 80°28′–80°38′W	Peatland	*Larch*, *Black spruce*, *Sphagnum* spp.	1990.6–1990.10	Moore et al., 1994
33	Quebec, Canada, NA	54°48′N, 66°49′W	Peatland	*Carex* spp.	1989.6–1989.9	Moore et al., 1990
34	Mississippi, USA, NA	34°24′N, 89°50′W	Marsh	*Carex hyalinolepis, Hydrocotyle umbellata, Festuca obtusa*	2005.5–2006.7	Koh et al., 2009
35	Sherman Island, USA, NA	38°2′N,121°45'W	Peatland	*Hordeum murinum L., Lepidium latifolium L.*	2009.4–2011.4 [*]	Hatala et al., 2012
36	Marcell forest, USA, NA	47°30′N,93°29'W	Peatland	*Carex spp., sphagnum moss, Eriophorum chamissonis, etc.*	2009–2010 [*]	Olson et al., 2013
37	Mer Bleue peatland, Canada, NA	45°41′N,75°48'W	Peatland	*Chamaedaphne calyculata, Ledum groenlandicum, etc.*	1999–2010 [*]	Moore et al., 2011
38	Sag riverside, Alaska, NA	69°30'N, 148°13' W	Peatland [a]	*Vascular plant, moss and a few short shrubs*	1996.6–1996.9 [*]	Harazono et al., 2006
39	Happy valley, Alaska, NA	69°10'N, 148°51'W	Peatland [a]	*Sphagnum moss, sedge*	1995.6–1995.9 [*]	Harazono et al., 2006
40	Churchill Manitoba, Canada, NA	58°40'N, 93°50'W	Peatland	*Carex aquatilis, Eriophorum spp., etc.*	2008–2010 [*]	Hanis et al., 2013
41	Northen Alaska, USA, NA	71°17′N, 156°36′W	Peatland	*Moss, Carex aquatilis, Eriophorum vaginatum, etc.*	2007.6–2007.8 [*]	Zona et al., 2009
42	Alberta, Canada, NA	54°57′N, 112°28′W	Peatland	*Picea mariana, Larix laricina, shrub etc.*	2007.5–2007.9 [*]	Long et al., 2010
43	Great Dismal Swamp, USA, NA	35°54′N, 76°09E	Swamp	*Taxodium distichum, Nyssa sylvatica, etc.*	2007.7–2009.6 [*]	Morse et al., 2012

[*] We used the reported average yearly CH_4 flux of the experimental year/period from the literature.
[&] Wetland sites used for calibration.
[$] These swamp sites do not have plant species information in the literature.
[a] Tundra.
[b] Tidal marsh.
[c] Mangrove.

Table 2. Model performance for $CH4MOD_{wetland}$ and the TEM for different continents and wetland types

Wetland type/Continent	$CH4MOD_{wetland}$								TEM								n
	R^2	RMSE	RMD	EF	CD	U_M	U_R	U_E	R^2	RMSE	RMD	EF	CD	U_M	U_R	U_E	
North America	0.82	75.37	-1.96	0.57	0.49	0.04	0.61	0.39	0.80	56.22	-2.86	0.76	1.59	0.00	0.03	0.97	28
Asia	0.94	55.79	-12.64	0.93	0.96	0.28	0.02	0.70	0.26	72.56	1.71	0.32	1.93	0.00	0.03	0.97	11
Europe	0.35	62.69	-32.60	0.15	1.13	0.27	0.03	0.69	NS	161.33	29.39	-4.65	0.34	0.03	0.84	0.13	13
South America/Africa	NS	57.32	39.52	-0.80	0.67	0.48	0.07	0.45	0.59	29.33	13.13	0.53	2.22	0.13	0.04	0.83	6
Marsh	0.75	29.44	0.52	0.22	0.37	0.00	0.73	0.27	NS	39.76	-18.77	-0.42	0.95	0.22	0.17	0.61	8
Peatland	0.83	82.26	-10.4	0.57	0.49	0.02	0.61	0.38	0.70	69.45	7.96	0.69	1.14	0.01	0.03	0.96	39
Swamp	0.50	74.28	43.07	0.13	0.54	0.34	0.19	0.47	0.76	40.76	19.02	0.74	1.27	0.22	0.03	0.75	7
Coastal wetland	0.80	55.46	-26.97	0.72	2.09	0.24	0.30	0.47	NS	188.26	101.00	-2.26	0.35	0.29	0.42	0.29	4
Global	0.81	67.00	4.28	0.65	0.59	0.00	0.45	0.54	0.68	63.58	4.63	0.68	1.46	0.01	0.01	0.98	58

NS represents no significant correlation

Table 3. CH_4 simulations by $CH4MOD_{wetland}$ and the TEM for different continents and wetland types. All units are Tg CH_4 yr^{-1} ± 1σ, where the standard deviation represents the interannual variation in the model estimates.

Continent/Wetland type	CH_4 Flux (g m^{-2} yr^{-1})		CH_4 Emissions (Tg)		Area (10^4 ×km^2)
	$CH4MOD_{wetland}$	TEM	$CH4MOD_{wetland}$	TEM	
Asia	23.27 ± 0.67	25.78 ± 0.14	25.37 ± 0.73	28.81 ± 0.15	109.04
Africa	27.64 ± 1.55	33.92 ± 0.27	21.12 ± 1.18	25.91 ± 0.20	76.39
N. America	11.48 ± 0.47	14.10 ± 0.18	24.38 ± 1.00	29.95 ± 0.38	212.35
S. America	29.61 ± 0.52	39.91 ± 0.54	26.24 ± 0.46	35.36 ± 0.48	88.60
Europe	7.77 ± 0.11	16.04 ± 0.28	6.48 ± 0.09	13.38 ± 0.23	83.40
Oceania	12.08 ± 2.52	11.31 ± 0.57	1.72 ± 0.27	1.61 ± 0.06	14.23
Lake, river *	15.57	15.57	27.32	27.32	175.46
Marsh	28.64 ± 1.06	39.60 ± 0.28	37.47 ± 1.39	51.80 ± 0.37	131.61
Peatland	1.99 ± 0.09	9.87 ± 0.27	0.42 ± 0.02	2.06 ± 0.06	21.00
Swamp	31.58 ± 0.57	45.59 ± 0.91	17.37 ± 0.32	25.08 ± 0.50	55.34
Coastal wetland	9.44 ± 0.25	11.63 ± 0.14	2.85 ± 0.08	3.51 ± 0.04	30.32
Intermittent wetland	18.49 ± 2.08	18.29 ± 0.19	5.81 ± 0.65	5.75 ± 0.06	31.60
No-specific wetland	10.21 ± 0.68	13.63 ± 0.25	14.07 ± 0.93	18.79 ± 0.34	138.67
Global	18.03 ± 0.49	23.00 ± 0.15	105.31± 2.72	134.31 ± 0.84	584.00

* IPCC Tier 1 method was used to estimate the CH_4 emissions from lakes and rivers. The CH_4 emission factor was from the IPCC (1996).

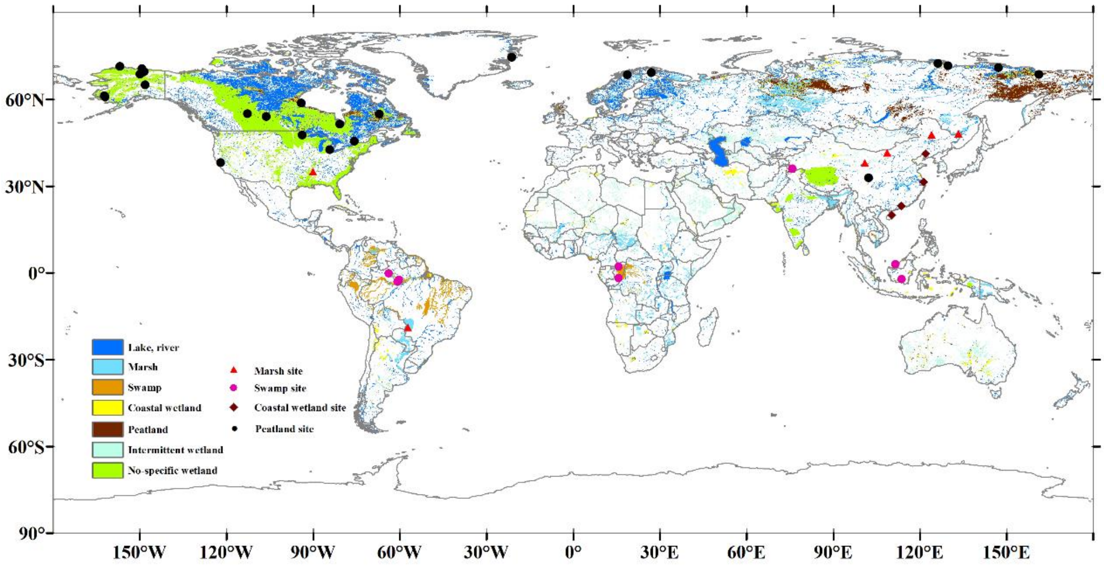

Figure 1: Wetland site distribution (Table 1) and global wetland maps of GLWD-3 (Lehner and Döll, 2004).

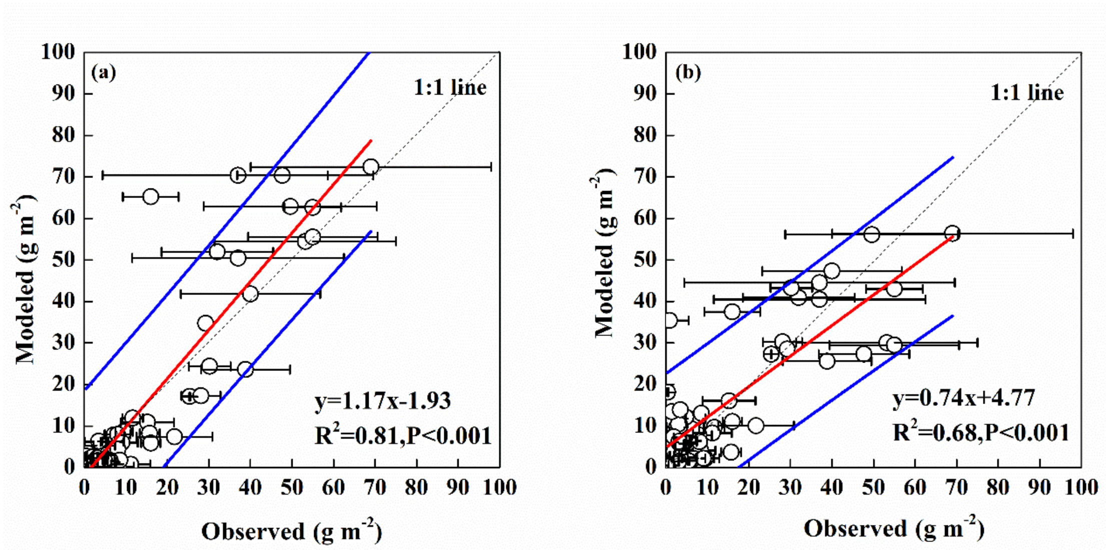

Figure 2: Regression of simulated against observed total amount of seasonal/annual CH_4 emissions from global wetland sites by $CH4MOD_{wetland}$ (a) and the TEM (b). The horizontal bars are the standard errors from the sampling replicates at the wetland site. The red line is the regression line of simulated vs. observed between modeled and observed values. The blue line is the prediction correspondence. The dashed line is the 1:1 line.

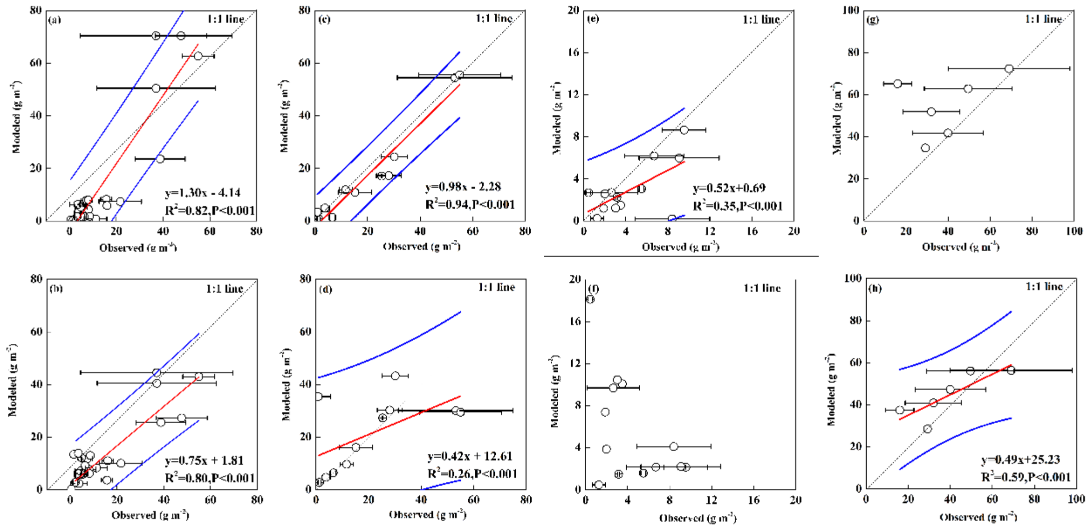

Figure 3: Regression of simulated against observed total amount of seasonal/annual CH_4 emissions from North American wetland sites by CH4MOD$_{wetland}$ (a) and the TEM (b), from Asian wetland sites by CH4MOD$_{wetland}$ (c) and the TEM (d), from European wetland sites by CH4MOD$_{wetland}$ (e) and the TEM (f), and from South American and African wetland sites by CH4MOD$_{wetland}$ (g) and the TEM (h). The horizontal bars are the standard errors from the sampling replicates at the wetland site. The blue line is the prediction correspondence. The dashed line is the 1:1 line.

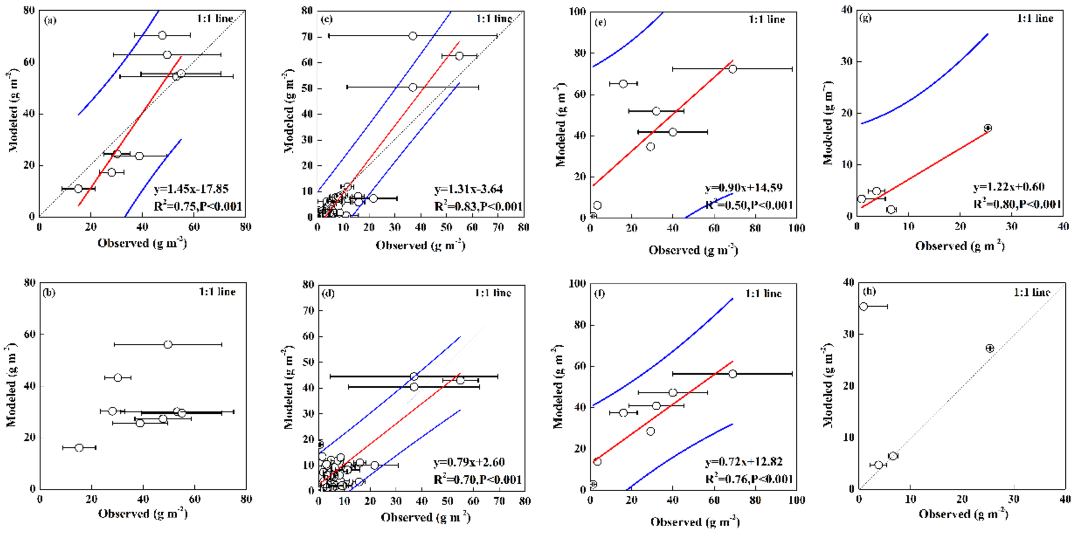

Figure 4: Regressions of simulated against observed total amount of seasonal/annual CH_4 emissions from marsh sites by $CH4MOD_{wetland}$ (a) and the TEM (b), from peatland sites by $CH4MOD_{wetland}$ (c) and the TEM (d), from swamp sites by $CH4MOD_{wetland}$ (e) and the TEM (f), and from coastal wetland sites by $CH4MOD_{wetland}$ (g) and the TEM (h). The horizontal bars are the standard errors from the sampling replicates at the wetland site. The blue line is the prediction correspondence. The dashed line is the 1:1 line.

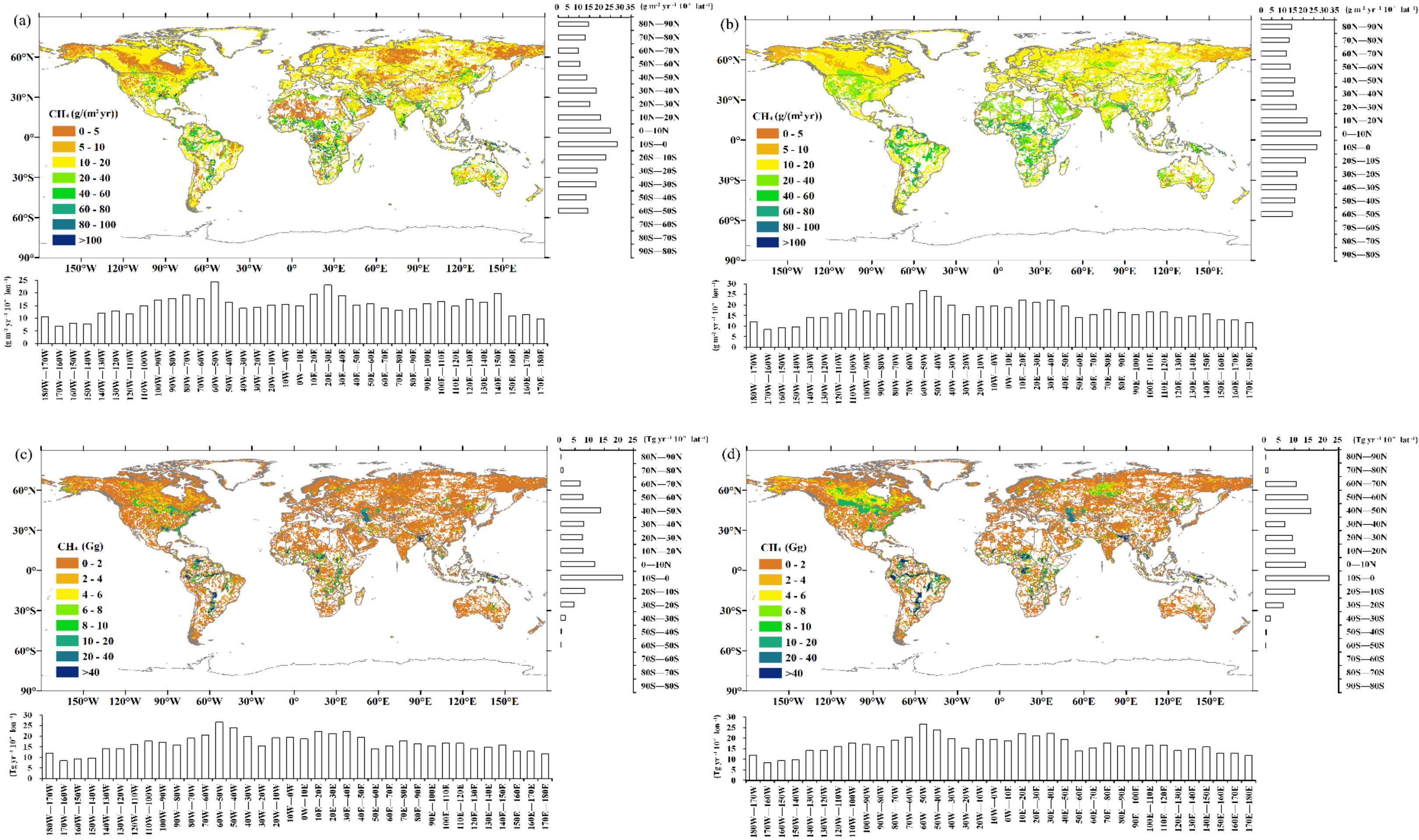

Figure 5: Spatial pattern of annual mean CH_4 fluxes for 2000–2010, with latitudinal and longitudinal distributions of annual mean CH_4 fluxes by $CH4MOD_{wetland}$ (a) and the TEM (b). Spatial pattern of annual mean CH_4 emissions for 2000–2010, with latitudinal and longitudinal distributions of annual mean CH_4 emissions by $CH4MOD_{wetland}$ (c) and the TEM (d). The CH_4 fluxes and emissions are aggregated in steps of 10°.